

AD A 049928

114 NORDA-REPORT 4

12

A NEW MODEL OF RESONANT ACOUSTIC
SCATTERING BY SWIMBLADDER - BEARING FISH.

10 RICHARD H. LOVE

9 FINAL rept. g

AD No. —
JDC FILE COPY

OCEAN ACOUSTICS DIVISION
NAVAL OCEANOGRAPHIC LABORATORY

11 AUGUST 1977



DDC
RECEIVED
FEB 14 1978
D
18 58p.

Approved for Public Release
Distribution Unlimited

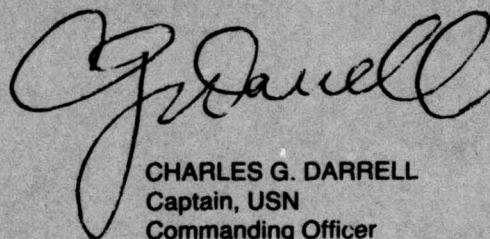
NAVAL OCEAN RESEARCH AND DEVELOPMENT ACTIVITY
NSTL Station, Mississippi 39529
392 773

Jell

FOREWORD

Oceanic volume reverberation can adversely affect the performance of Navy sonars. Small swimbladder-bearing fish are the primary cause of this reverberation at ship sonar frequencies. This report describes a new acoustic model of a swimbladder-bearing fish. This model is an improvement over previous models and should be of value in future volume reverberation studies.

This report was originally a dissertation submitted in partial fulfillment of the requirements for the Ph.D. degree in acoustics at the Catholic University of America.



CHARLES G. DARRELL
Captain, USN
Commanding Officer
NORDA

ACCESSION FOR	
NTIS	White Section <input checked="" type="checkbox"/>
DDC	Diff Section <input type="checkbox"/>
UNANNOUNCED	<input type="checkbox"/>
JUSTIFICATION	
BY	
DISTRIBUTION/AVAILABILITY CODES	
Dist.	AVAIL. and/or SPECIAL
A	

EXECUTIVE SUMMARY

A new model of a swimbladder-bearing fish has been developed in order to provide improved predictions of the resonant frequency and acoustic cross section of such a fish. The model consists of a small spherical shell in water, enclosing an air cavity which supports a surface tension. The shell is a viscous, heat-conducting Newtonian fluid, with the physical properties of fish flesh. A comparison of the results obtained with the new model to experimental data indicates that the new model constitutes a definite improvement over previous models. The new model can predict the high values of damping and elevated resonant frequencies that previous models could not. The model appears to be most accurate for fish in which tension in the swimbladder wall has a minor effect on resonant scattering. This includes the fish which are of interest in studies of volume reverberation and therefore, the new model should be of considerable value in such studies.

DDC
 RECEIVED
 FEB 14 1978
 D

EXECUTIVE SUMMARY

ACKNOWLEDGMENTS

It is my pleasure to acknowledge the guidance and advice provided by Dr. Thomas J. Eisler. My appreciation also goes to Drs. Ronald New and John J. McCoy for their critical review of the manuscript. Special thanks go to Mr. Robert S. Winokur, for his cooperation and support throughout the course of this work.

CONTENTS

	Page
I. INTRODUCTION	1
Volume Reverberation	1
Existing Models	2
Experimental Data	4
II. A NEW MODEL	7
The Model	7
Limits and Physical Properties	7
Formulation of Equations	8
Boundary Conditions	16
III. SOLUTION	19
IV. DISCUSSION	23
Results	23
Comparison to Free Bubble	25
Comparison to Experimental Data	28
V. CONCLUSIONS	33
REFERENCES	35
APPENDIX A: Physical Properties of Fish	37
APPENDIX B: Simplified Expression for (B_w/A)	42

LIST OF ILLUSTRATIONS

Figure 1.	Resonant frequency of a prolate spheroidal bubble	5
Figure 2.	Resonant frequency of the new model of a swimbladder-bearing fish	24
Figure 3.	Viscous and radiation damping factors for the new model of a swimbladder-bearing fish	26
Figure 4.	Thermal damping factors for the new model of a swimbladder-bearing fish	27

LIST OF TABLES

Table I.	Physical Properties	8
Table II.	Experimental Data and Results of Comparisons to the New Model	29

CHAPTER I

INTRODUCTION

Volume Reverberation

When sound is propagated in the ocean any inhomogeneities in the medium will scatter a portion of the sound incident upon them. This scattered sound is termed volume reverberation. If volume reverberation levels are high, the operation of an active sonar can be adversely affected. Specifically, high reverberation levels can mask an echo reflected from a particular target of interest.

During World War II, researchers studying sonar echo ranging at the University of California Division of War Research (UCDWR) discovered that volume reverberation levels were usually vertically stratified. Layers of high reverberation, on the order of 100 m thick, were found, usually within the upper 1,000 m of the water column, extending over large geographic areas of the Pacific Ocean [1,2]. Other researchers subsequently found such layers in other oceans [3,4]. These layers came to be known as deep scattering layers (DSL). In addition, it was found that these layers frequently rose to shallower depths around sunset and descended around sunrise. This gave rise to the hypothesis that deep scattering layers were caused by biological organisms, which were known to undergo diurnal vertical migrations [5].

The great difference between the acoustic impedances of air and sea water causes an air bubble to be a much more effective scatterer than other objects of comparable size [6]. This fact led Marshall to examine the possibility that small mid-water fish which contained air-filled swimbladders were the cause of DSL [7]. His study strongly implicated such fish as major components of DSL. The primary scattering mechanism was considered to be swimbladders which could resonate in the fundamental, or volume pulsation, mode when insonified at the proper frequency. Subsequent research by Hersey and co-workers displayed the frequency dependence of reverberation levels and provided further qualitative proof that resonant scattering by swimbladder-bearing fish was the major cause of volume reverberation in the ocean [8-11]. The study of volume reverberation in the world ocean has continued (for example, see reference 12) and it is now generally accepted that swimbladders of fish are the predominant scattering mechanism in most geographic areas. However, it has not been until very recently that quantitative comparisons between fish distribution data and acoustic volume reverberation data have been made.

The fundamental volume reverberation parameter is the back-scattering coefficient of a unit volume of ocean, M , which is the ratio of the scattered intensity at a unit distance from the unit volume, I_s , to the incident intensity, I_i , [13],

$$M = I_s / I_i \quad (I-1)$$

If it is assumed that the scattered signals add incoherently [13], then M can be defined in terms of the scatterers as

$$M = \frac{1}{4\pi V} \sum_{j=1}^n \sigma_j \quad (I-2)$$

where n is the number of scatterers in volume V and σ_j is the ratio of scattered power to incident intensity of the j th scatterer. σ is called the acoustic cross section of the scatterer.

Although M is the fundamental parameter, the quantity which is most often utilized in any discussion of volume reverberation is the scattering strength per unit volume, S_v , which is M expressed in decibels.

$$S_v = 10 \log M \quad (I-3)$$

S_v is often simply called scattering strength [14].

In any acoustic measurement of volume reverberation, S_v is obtained basically from the equation

$$S_v = 10 \log (I_s / I_i) \quad (I-4)$$

The determination of I_i and I_s is relatively straightforward and acoustic measurements of S_v are fairly routine. However, if a determination of S_v is to be made from the distribution of scatterers, the equation employed is

$$S_v = 10 \log \left[\frac{1}{4\pi V} \sum_{j=1}^n \sigma_j \right] \quad (I-5)$$

The difficulty in making quantitative comparisons between acoustic measurements of volume reverberation and the distribution of swimbladder fishes lies in the determination of both n and σ . The determination of the number of fish and the species, size and swimbladder size of each is strictly a biological problem which will not be considered here. However, the difficulty of this problem is not to be minimized. Given the size and swimbladder size of an individual fish, calculation of σ is also difficult, due to the complex structure of fish.

Simplified models have been developed in order to estimate σ near resonance for an individual fish. These models are based on the premise that only the swimbladder is a significant contributor to σ near resonance. Experimental evidence [15] shows, in fact, that this is so, whereas, at frequencies much higher than the resonant frequency, the swimbladder and the body of the fish contribute about equally to σ [16].

Experimental evidence indicates that the existing models have some shortcomings. After a review of the models and the experimental data, it will be the purpose of this report to develop an improved model of resonant scattering from an individual swimbladder-bearing fish in order to eliminate or at least decrease the shortcomings of the existing models.

Existing Models

A swimbladder is essentially just an air bubble within the fish, so that the simplest acoustic model of a swimbladder fish is an ideal spherical air bubble having the same volume as the swimbladder. The frequency of the fundamental mode of resonance of a small ideal spherical air bubble in water was determined by Minnaert [17] to be

$$\omega_0^2 a^2 = \frac{3\gamma_a P_0}{\rho_{0w}}, \quad (I-6)$$

where ω_0 is the circular frequency of resonance, a the equilibrium bubble radius, P_0 the ambient pressure, γ_a the ratio of specific heats of air, and ρ_{0w} the density of water. The acoustic cross section of a small ideal spherical air bubble in water is [18]

$$\sigma = \frac{4\pi a^2}{\left(\frac{\omega_0^2}{\omega^2} - 1\right)^2 + \frac{\omega^2 a^2}{c_w^2}}, \quad (I-7)$$

where ω is the insonifying frequency and c_w is the sound velocity in water. The limiting factor on these equations is the size of the bubble, which is limited to values such that $(\omega a/c_w) \ll 1$.

For a small real air bubble in water, the above equations for ω_0 and σ remain the same, except that the term $(\omega^2 a^2/c_w^2)$ in equation I-7 is replaced by d^2 [18]. d is an unspecified damping constant which includes the effects of heat conduction, surface tension, viscosity, and other processes.

Devin [19] studied the damping at resonance of real air bubbles in water. He found that the damping constant at resonance, δ , was the sum of three damping processes: thermal damping, δ_{th} , viscous damping, δ_{vis} , and radiation damping, δ_{rad} .

$$\delta = \delta_{rad} + \delta_{vis} + \delta_{th}. \quad (I-8)$$

δ is defined such that, at $\omega = \omega_0$, $d = \delta$. Devin determined the values of δ_{rad} , δ_{vis} , and δ_{th} , for bubbles of the size which are of present interest, to be

$$\delta_{rad} = \frac{\omega_0 a}{c_w}, \quad (I-9)$$

$$\delta_{vis} = \frac{4\eta_{sw}}{\rho_{0w}\omega_0 a^2}, \quad (I-10)$$

$$\delta_{th} = \frac{3(\gamma_a - 1)}{a} \left(\frac{\kappa_a}{2\omega_0 \rho_{0a} c_{pa}} \right)^{1/2}, \quad (I-11)$$

where η_{sw} is the shear viscosity of water, κ_a is the thermal conductivity of air, ρ_{0a} is the density of air, and c_{pa}

is the specific heat at constant pressure for air. Eller [20] extended these results to non-resonant frequencies. However, Fairbank [21] has recently contended that Eller's results are incorrect by a factor of $(\omega_0/\omega)^2$.

A progression of improvements have been made to Minnaert's original work, which has included such effects as compressibility, surface tension, and viscosity [22-24]. The resonant frequency of a spherical air bubble in water where the effects of surface tension and viscosity are included is [23]

$$\omega_0^2 a^2 = \frac{3\gamma_a P_0}{\rho_{0w}} - \frac{4\eta_{sw}^2}{\rho_{0w}^2 a^2} + \frac{2s(3\gamma_a - 1)}{\rho_{0w} a}, \quad (I-12)$$

where s is the surface tension. In all of the above references the bubble-water system was modeled as a spring-mass system and the effect of viscosity included in the damping term. Hsieh [25] maintains that this method of including viscous effects is adequate only so long as the damping is small.

In an attempt to improve on the air bubble in water as a model of scattering from a swimbladder fish, Andreeva [26] developed a model of an air bubble in an infinite elastic medium. This elastic medium was described by a complex shear modulus, μ_r ,

$$\mu_r = \mu_{r1} + i\mu_{r2} \quad (I-13)$$

It has been determined that, for fish flesh [27]

$$10^5 \text{ dynes/cm}^2 \leq \mu_{r1} \leq 10^7 \text{ dynes/cm}^2,$$

and

$$0.2 \mu_{r1} \leq \mu_{r2} \leq 0.3 \mu_{r1}.$$

Andreeva chose $\mu_{r1} = 10^6 \text{ dynes/cm}^2$ and all other properties of the elastic medium were set equal to those of water.

Using this model, Andreeva obtained the following equations for the resonant frequency and acoustic cross section at resonance of a small, spherical bubble:

$$\omega_0^2 a^2 = \frac{3\gamma_a P_0 + 4\mu_{r1}}{\rho_{0f}} \quad (I-14)$$

and

$$\sigma = \frac{4\pi a^2}{\left(\frac{\omega_0^2}{\omega^2} - 1\right)^2 + \left(\frac{\omega_0^2}{\omega^2 Q^2}\right)} \quad (I-15)$$

where Q defines the sharpness of the resonance peak. Q is termed the damping factor and is defined at $\omega = \omega_0$ to be

$$Q = \frac{\omega_0}{\omega_2 - \omega_1} = \frac{1}{\delta} \quad (I-16)$$

where ω_1 and ω_2 are the frequencies at which the scattered sound power is one-half that at ω_0 [19].

Andreeva has utilized Devin's [19] work to obtain values for Q .

Thus

$$\frac{1}{Q_{\text{rad}}} = \frac{\omega_0 a}{c_f}, \quad (I-17)$$

$$\frac{1}{Q_{\text{vis}}} = \frac{4\mu_{r2}}{\rho_{0f} \omega_0^2 a^2}, \quad (I-18)$$

and

$$\frac{1}{Q_{\text{th}}} = \frac{3(\gamma_a - 1)}{a} \left(\frac{\kappa_a}{2\omega_0 \rho_{0f} c_{pa}} \right)^{1/2}. \quad (I-19)$$

Q was calculated by Andreeva to vary between 5 and 10, the value varying with depth. Equations I-17 and I-19 are equivalent to equations I-9 and I-11.

Equation I-14 reduces to the resonant frequency of an air bubble in water (equation I-6) as μ_{r1} approaches zero. In addition, if P_0 approaches zero, that is, if the air were evacuated from the sphere, equation I-14 reduces to the resonant frequency of a spherical cavity in rubber [28].

Equation I-15 is actually defined only at resonance because Q is defined only at resonance. However, for the values of Q obtained by Andreeva, the Q -term is significant only near resonance. Therefore, although the equation is not strictly defined away from resonance, it can be used equally well at or off resonance.

Lebedeva [29] improved Andreeva's model by considering an air-bubble inside an elastic shell in water and by extending the results to off-resonance cases. However, thermal losses were neglected. For this model,

$$\omega_0^2 a^2 = \frac{3\gamma_a P_0}{\rho_{0f}} + \frac{4\mu_{rf}}{\rho_{0f}} \left(1 - \frac{a^3}{b^3}\right) \quad (I-20)$$

and

$$\sigma = \frac{4\pi a^2}{\left[\frac{\omega_0^2}{\omega^2} - 1\right]^2 + \left[\frac{\omega a}{c_f} + \frac{4\mu_{rf}}{\rho_{0f}\omega^2 a^2} \left(1 - \frac{a^3}{b^3}\right)\right]^2}, \quad (I-21)$$

where b is the outside radius of the shell. Thus for $a^3/b^3 < 1$, equation I-20 is equivalent to equation I-14. Equation I-21 can be written in the form of equation I-15 as

$$\sigma = \frac{4\pi a^2}{\left(\frac{\omega_0^2}{\omega^2} - 1\right)^2 + \left(\frac{\omega_0^2}{\omega^2 H^2}\right)}, \quad (I-22)$$

where, at $\omega = \omega_0$, $H = Q$ such that,

$$\frac{1}{H_{rad}} = \frac{\omega^2 a}{\omega_0 c_f} \quad (I-23)$$

and

$$\frac{1}{H_{vis}} = \frac{4\mu_{rf}}{\rho_{0f}\omega\omega_0 a^2} \left(1 - \frac{a^3}{b^3}\right). \quad (I-24)$$

In all of the above studies only the fundamental, volume pulsation, mode has been considered and all higher modes have been neglected. Strasberg [30] has shown that appreciable sound is radiated from a bubble only when it is oscillating in the fundamental mode and the sound radiation associated with higher modes is several orders of magnitude lower. On this basis, it is evident the consideration of only the fundamental mode is reasonable, and therefore only the fundamental mode will be considered in this report.

In addition, all of the studies have assumed a spherical bubble or swimbladder. However, swimbladders generally are not spherical in shape. They usually more closely resemble prolate spheroids, with minor- to major-axis ratios, ϵ , generally ranging between 0.1 and 0.5 [6,31-33]. Strasberg [34] and Weston [35] have shown that spheroidal bubbles have a resonant frequency only slightly higher than spherical bubbles of the same volume. For a prolate spheroidal bubble, the resonant frequency $\omega_{0\epsilon}$, is [35]

$$\frac{\omega_{0\epsilon}}{\omega_0} = \zeta = \frac{2^{1/2}(1 - \epsilon^2)^{1/4}}{\epsilon^{1/2}} \left\{ \ln \left[\frac{1 + (1 - \epsilon^2)^{1/2}}{1 - (1 - \epsilon^2)^{1/2}} \right] \right\}^{-1/2}. \quad (I-25)$$

(It should be noted that this equation is printed incorrectly in reference 35.) Equation I-25 is plotted in Figure 1. The assumption that the swimbladder shape can be modeled by a sphere is a reasonable one for $1 \leq \epsilon^{-1} \leq 4$, where $1 \leq \zeta \leq 1.1$, and is not really grossly in error at an extreme ϵ^{-1} of 20, where $\zeta = 1.4$.

Weston [35] has presented a comprehensive review of scattering, covering the information available to 1966. Although a specific scattering model is not presented, many aspects of scattering from a fish with a gas-filled swimbladder are discussed.

Experimental Data

Several sets of experimental measurements of the acoustic characteristics of swimbladder fish near resonance have been conducted. Some measurements have been conducted for the purpose of studying the effect of fish on the propagation and scattering of sound in the ocean and others have been conducted in connection with studies on fish sound production and hearing.

The first experimental work was conducted by Coate [36]. In a short series of measurements on a dead 20-cm long crappie, he determined that a spherical air bubble in water was a reasonable model for resonant scattering from a swimbladder, provided that an arbitrary loss term was included. The magnitude and form of this loss term were left unspecified.

Batzler and Pickwell [15] made measurements on several live goldfish and anchovies, which were 6- to 11-cm long. The experimental resonant frequencies were found to agree well with those predicted by equation I-14 if a value of 5×10^5 dynes/cm² were used for μ_{rf} . However, measured Q 's were in the range of 3 to 5, which are lower than predicted by Andreeva.

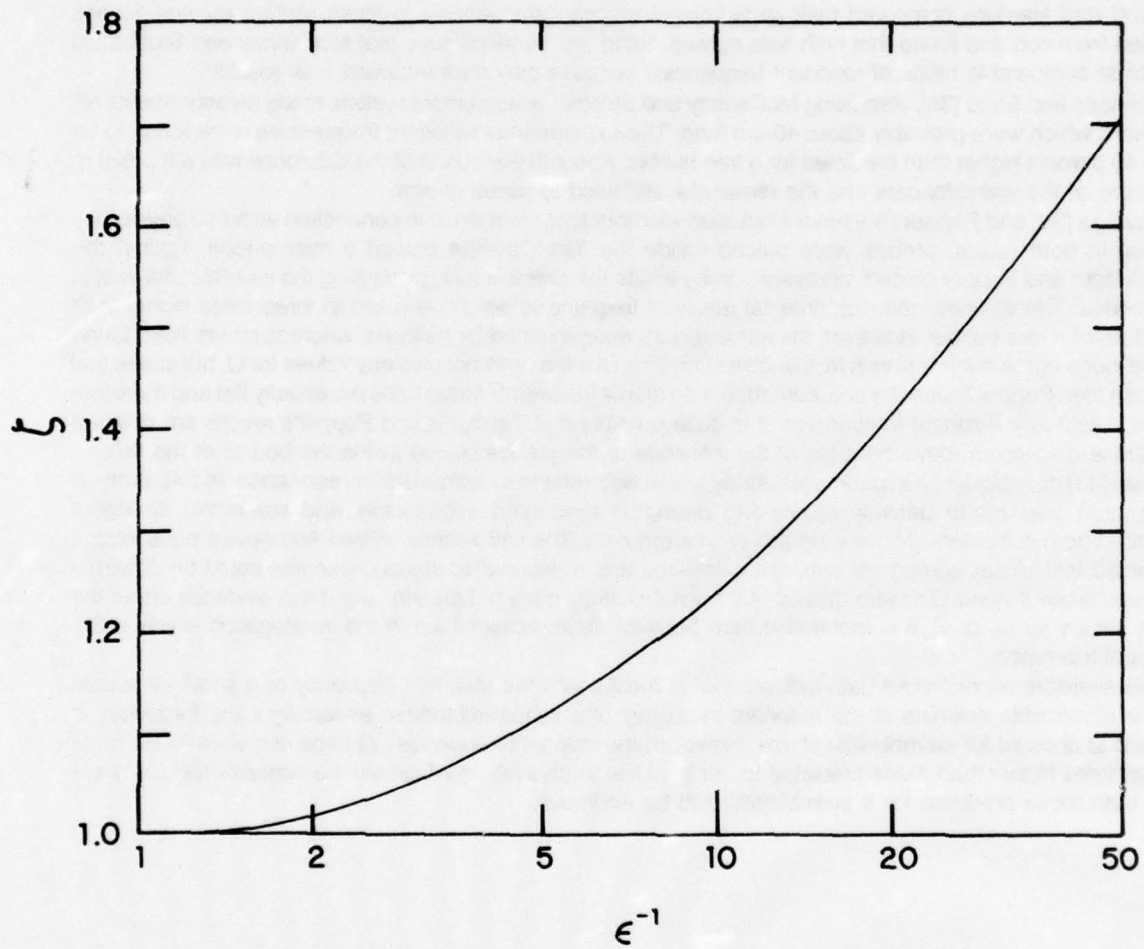


FIGURE 1. RESONANT FREQUENCY OF A PROLATE SPHEROIDAL BUBBLE

McCartney and Stubbs [37] made measurements on live cod, saithe, and pollack, which were 30- to 55-cm long. The experimental resonant frequencies were found to be 40 to 100 percent higher than those predicted for a free bubble and about 15 to 60 percent higher than those predicted by Andreeva. The differences were attributed to the nonspherical shapes of the swimbladders and to tension in swimbladder tissues. Again, measured Q's were lower than those predicted by Andreeva, having values of about 1 to 3.5.

Sand and Hawkins [33], using McCartney and Stubbs' measurement system, made measurements on live cod which were 13- to 50-cm long. When the fish were at a depth at which they had been allowed to adapt for several days, the experimental resonant frequencies were found to be from about 25 to 600 percent higher than those predicted for a free bubble and the measured Q's were approximately 1. The ratio of the experimental resonant frequency to that of a free bubble was found to generally increase with increasing fish size. Sand and Hawkins suggest that the cod maintained a tension in the swimbladder wall, which raised the experimental resonant frequencies.

Sand and Hawkins compared their experimental resonant frequencies to those McCartney and Stubbs obtained from cod and found that both sets agreed. Sand and Hawkins state that McCartney and Stubbs did not obtain comparable ratios of resonant frequencies because they misinterpreted their results.

Sundnes and Sand [38], also using McCartney and Stubbs' measurement system, made measurements on live charr, which were probably about 40-cm long. The experimental resonant frequencies were found to be about 40 percent higher than predicted for a free bubble. About three-fourths of the difference was attributed to the shape of the swimbladders and the remainder attributed to tissue effects.

Tavolga [39] and Popper [40] have examined swimbladder resonance in connection with fish physiology studies. In both cases, probes were placed inside the fish. Tavolga placed a microphone against the swimbladder and Popper placed a pressure probe inside the swimbladder, puncturing the swimbladder wall in the process. Tavolga obtained experimental resonant frequencies which were two to three times higher than predicted for a free bubble. However, the same results were obtained for balloons, whereas others have found that balloons agree quite well with free bubbles [15, 37]. Tavolga does not give any values for Q, but states that it is quite low. Popper found the pressure response inside the swimbladder to be essentially flat and therefore did not obtain any resonant frequencies. It is quite possible that Tavolga's and Popper's results are different from those discussed above because of the influence of the probes placed inside the bodies of the fish.

Love [41] conducted an experimental study which was related to swimbladder resonance. In this study, a comparison was made between scattering strengths measured acoustically and scattering strengths calculated from coincidentally collected fish distribution data. The calculations utilized Andreeva's equations. It was noted that closer agreement between calculated and measured scattering strengths could be obtained near resonance if lower Q's were utilized. Although this study does not present any direct evidence about the proper values for ω_0 or Q, it is mentioned here because its implications led to the investigation which is the subject of this report.

The available experimental data indicate that in most cases the resonant frequency of a small air bubble gives a reasonable estimate of the resonant frequency of a fish swimbladder, especially if the frequency is adjusted to account for swimbladder shape. However, the resonant frequencies of large cod were found to be several times higher than those predicted for air bubbles. In addition, in all cases, the experimental Q's were lower than those predicted for a swimbladder fish by Andreeva.

CHAPTER II

A NEW MODEL

The Model

The purpose of this report is to improve the equations which are presently utilized to predict the resonant frequency and acoustic cross section of a swimbladder fish, in order to facilitate the correlation of acoustic and biological volume reverberation data. A new model for a swimbladder fish is proposed and the appropriate equations developed for it. The model consists of a small spherical shell, enclosing an air cavity, in water. The shell is chosen to be a viscous, heat-conducting Newtonian fluid, with the physical properties of fish flesh, and the interface between the shell and the cavity supports a surface tension.

The shell is insonified by a harmonic plane compressional wave whose wavelength is large compared to the shell diameter. For convenience, the center of the shell will be taken as the origin of the coordinate system and the wave will travel in the positive direction along the z-axis. Spherical coordinates (r, θ, ϕ) will be used to describe the field, where r is the distance from the origin, θ the polar angle and ϕ the azimuthal angle. Since the problem is axisymmetric, $\partial/\partial\phi = 0$.

Acoustically, fish flesh may be considered to resemble soft rubber. In such a substance, shear waves are much less important than transverse waves and the substance can be closely approximated by a viscous fluid. Modelling fish flesh as a viscous liquid has advantages over modelling it as an elastic solid with a complex shear modulus. Specifically, exact equations (Navier-Stokes) exist for the motion of viscous fluids, whereas a phenomenological approach is required if a complex shear modulus is utilized.

The body of a fish which surrounds its swimbladder will cause an increase in stiffness over that of a free bubble. It is assumed that most of that increased stiffness is concentrated in the swimbladder wall and may be modelled by a surface tension at that interface. Unlike an elastic modulus, swimbladder tension may be under the fish's control and could account for otherwise unexpected variations in resonant frequency.

Limits and Physical Properties

Several limits will be placed on this model. These include limits on applicable depth, frequency, and size ranges. The depth range of interest is from the surface to 1,000 m, which corresponds to an ambient pressure of 10^6 to 10^8 dynes/cm². The frequency range is 100 Hz to 40 kHz, which corresponds to a circular frequency, ω , of $2\pi \times 10^2$ to $8\pi \times 10^4$ rad/sec. The fish size range is 1 cm to 1 m. This roughly corresponds to an inner shell radius, a , of 10^{-1} to 5 cm. (Appendix A contains a discussion of swimbladder volumes.) The ratio of outer shell radius, b , to a is $2.5 \leq b/a \leq 6$ for small fish and $2.5 \leq b/a \leq 3.2$ for large fish. Two further limitations will be that 6×10^2 cm/sec $\leq \omega a \leq 2.4 \times 10^4$ cm/sec and that $\omega b \leq 7 \times 10^4$ cm/sec.

In addition to swimbladder size, the surface tension at the swimbladder wall must be specified. For small fish,

$$10^2 \text{ dyne/cm} \leq s \leq 10^6 \text{ dyne/cm}$$

and for large fish,

$$10^2 \text{ dyne/cm} \leq s \leq 10^9 \text{ dyne/cm}.$$

The rationale for this choice of ranges is discussed in Appendix A.

Several other parameters must also be specified. These include the velocity of a compressional wave (sound velocity), c ; density, ρ_0 ; specific heat at constant pressure, c_p ; ratio of specific heats, γ ; thermal conductivity, κ ; shear viscosity, η_s ; and bulk viscosity η_b ; for air, sea water, and fish flesh. Subscripts a , w , and f will be utilized to indicate the properties of air, sea water, and fish flesh, respectively. For convenience, a viscosity parameter, ξ , is defined as

$$\xi = \frac{4}{3}\eta_{sf} + \eta_{bf}. \quad (\text{II-1})$$

The parameters are listed in Table 1, for a temperature of 10°C and, unless specified, a pressure of one atmosphere (10^6 dyne/cm²). The properties of air were obtained from references 42 and 43 and those of sea water from reference 44. The properties of fish flesh are discussed in Appendix A.

Table 1 — Physical Properties

	Air	Sea Water	Fish Flesh
c , cm/sec	3.3×10^4	1.50×10^5	1.55×10^5
ρ_0 , gm/cm ³	1.3×10^{-3} (at 1 atm) 1.3×10^{-1} (at 100 atm)	1.026	1.050
γ	1.40	1.01	1.01
C_p , $\frac{\text{cal}}{\text{gm } ^\circ\text{C}}$	0.24	0.93	0.89
κ , $\frac{\text{cal}}{\text{cm sec } ^\circ\text{C}}$	5.5×10^{-5}	1.34×10^{-3}	1.32×10^{-3}
η_s , poise	1.8×10^{-4}	1.4×10^{-2}	
ξ , poise			1 to 10^4

Preliminary analysis of the new model indicated that considerable simplification resulted, with virtually no loss of accuracy, if several approximations were made concerning the physical properties. The first approximations were that $\gamma_w = \gamma_f = 1$. Secondly, since $\kappa_w \approx \kappa_f \gg \kappa_a$, it was assumed that any heat generated in the air is rapidly conducted away, so that the temperature in fish flesh and water is constant. Thirdly, since $\eta_{sf} \gg \eta_{sw} \gg \eta_{sa}$, it was assumed that $\eta_{sw} = \eta_{sa} = 0$.

One further assumption which greatly simplifies the problem is made in this model. As discussed in Chapter I, only the fundamental, or zeroth mode of oscillation will be considered.

Formulation of Equations

The first step in the determination of the resonant frequency and acoustic cross section of the new model is the determination of the proper wave equations in water, fish flesh, and air. The wave equations are determined from the basic equations of motion as given by Hunt [45], generally following the method discussed by Epstein and Carhart [46]. The basic equations are the continuity equation,

$$\frac{\partial \rho}{\partial t} + \nabla \cdot (\rho \bar{u}) = 0 ; \quad (\text{II-2})$$

the equation of conservation of momentum,

$$\rho \frac{\partial \bar{u}}{\partial t} = -\rho(\bar{u} \cdot \nabla)\bar{u} - \nabla P + \xi \nabla(\nabla \cdot \bar{u}) - \eta_s \nabla \times (\nabla \times \bar{u}) ; \quad (\text{II-3})$$

the equation of conservation of energy,

$$\rho c_v \left(\frac{\partial T}{\partial t} + \bar{u} \cdot \nabla T \right) + \frac{\rho(c_p - c_v)}{\beta} \nabla \cdot \bar{u} + \nabla \cdot \bar{q} - \phi_v = 0 ; \quad (\text{II-4})$$

and the equation of state,

$$\rho = \rho(P, T) ; \quad (\text{II-5})$$

where ρ is density, t is time, \bar{u} is a velocity vector, P is pressure, c_v is specific heat at constant volume, T is absolute temperature, β is the coefficient of thermal expansion, \bar{q} is a heat conduction flux vector,

$$\bar{q} = -\kappa \nabla T , \quad (\text{II-6})$$

and ϕ_v is a viscous dissipation function.

Equations II-2 through II-5 are linearized by assuming that

$$\bar{u} = 0 + \bar{u}_1, \quad (II-7)$$

$$\rho = \rho_0 + \rho_1, \quad (II-8)$$

$$T = T_0 + T_1, \quad (II-9)$$

and

$$P(\rho, T) = P_0(\rho_0, T_0) + P_1, \quad (II-10)$$

where the subscripts 0 and 1 refer to the average and perturbation values of the parameters, respectively. The first-order equations are

$$-\frac{\partial \rho_1}{\partial t} + \rho_0 (\nabla \cdot \bar{u}_1) = 0, \quad (II-11)$$

$$\rho_0 \frac{\partial \bar{u}_1}{\partial t} = -\nabla P_1 + \xi \nabla (\nabla \cdot \bar{u}_1) - \eta_s \nabla \times (\nabla \times \bar{u}_1), \quad (II-12)$$

$$\rho_0 c_v \frac{\partial T_1}{\partial t} + \rho_0 \frac{(c_p - c_v)}{\beta} \nabla \cdot \bar{u}_1 - \kappa \nabla^2 T_1 = 0, \quad (II-13)$$

since ϕ_v is of second order [45], and

$$\rho_1 = \left(\frac{\partial \rho_0}{\partial P_0} \right)_T P_1 + \left(\frac{\partial \rho_0}{\partial T_0} \right)_P T_1. \quad (II-14)$$

It has been assumed that $T_{1f} = T_{1w} = 0$ and that $\gamma_f = \gamma_w = 1$. Hence, in fish flesh, equations II-11 through II-14 are

$$\frac{\partial \rho_{1f}}{\partial t} + \rho_{0f} (\nabla \cdot \bar{u}_1) = 0, \quad (II-15)$$

$$\rho_{0f} \frac{\partial \bar{u}_1}{\partial t} = -\nabla P_1 + \xi \nabla (\nabla \cdot \bar{u}_1) - \eta_{sf} \nabla \times (\nabla \times \bar{u}_1), \quad (II-16)$$

and

$$\rho_{1f} = \left(\frac{\partial \rho_{0f}}{\partial P_0} \right)_T P_1. \quad (II-17)$$

These equations are the same in water, with the exception that the viscosity is set to zero. The isothermal compressibility, K_T , is defined as

$$K_T = \frac{1}{\rho_0} \left(\frac{\partial \rho_0}{\partial P_0} \right)_T, \quad (II-18)$$

and the adiabatic sound velocity, c , as

$$c^2 = \frac{\gamma}{\rho_0 K_T}. \quad (II-19)$$

Since $\gamma_f = \gamma_w = 1$, equation II-17 is

$$\rho_{1f} = \frac{P_1}{c_f^2} \quad (II-20)$$

and equation II-15 is

$$\frac{\partial P_1}{\partial t} + \rho_{0f} c_f^2 (\nabla \cdot \bar{u}_1) = 0. \quad (II-21)$$

According to Helmholtz's theorem [47], the \bar{u}_1 vector field can be represented in terms of a vector potential \bar{A} and a scalar potential Ω such that

$$\bar{u}_1 = \nabla \times \bar{A} - \nabla \Omega, \quad (II-22)$$

$$\text{with } \nabla \cdot \bar{A} = 0, \quad (II-23)$$

$$\text{so that } \nabla \cdot \bar{u}_1 = -\nabla^2 \Omega, \quad (II-24)$$

$$\text{and } \nabla \times \bar{u}_1 = -\nabla^2 \bar{A}. \quad (II-25)$$

Thus, equations II-21 and II-16 become

$$\rho_{0f} c_f^2 \nabla^2 \Omega = \frac{\partial P_1}{\partial t} \quad (II-26)$$

and

$$\rho_{0f} \frac{\partial}{\partial t} (\nabla \times \bar{A}) - \eta_{sf} \nabla \times (\nabla^2 \bar{A}) = -\nabla P_1 - \xi \nabla (\nabla^2 \Omega) + \rho_{0f} \frac{\partial}{\partial t} (\nabla \Omega). \quad (II-27)$$

If the curl of equation II-27 is taken,

$$\nabla \times \nabla P_1 = \nabla \times \nabla \Omega = \nabla \times \nabla (\nabla^2 \Omega) = 0. \quad (II-28)$$

Thus,

$$\rho_{0f} \frac{\partial}{\partial t} (\nabla \times \bar{A}) - \eta_{sf} \nabla \times (\nabla^2 \bar{A}) = 0, \quad (II-29)$$

or

$$\eta_{sf} \nabla^2 \bar{A} - \rho_{0f} \frac{\partial \bar{A}}{\partial t} = 0. \quad (II-30)$$

Therefore,

$$\nabla P_1 + \xi \nabla (\nabla^2 \Omega) - \rho_{0f} \frac{\partial}{\partial t} (\nabla \Omega) = 0. \quad (II-31)$$

Then substituting equation II-26 into II-31 and taking the divergence yields:

$$\nabla^2 P_1 + \frac{\xi}{\rho_{0f} c_f^2} \nabla^2 \left(\frac{\partial P_1}{\partial t} \right) - \frac{1}{c_f^2} \frac{\partial^2 P_1}{\partial t^2} = 0. \quad (II-32)$$

Equations II-30 and II-32 are the wave equations in the fish flesh. In water, where the viscosity is zero, the wave equation is

$$\nabla^2 P_1 - \frac{1}{c_w^2} \frac{\partial^2 P_1}{\partial t^2} = 0. \quad (II-33)$$

The harmonic time dependence is now introduced, such that

$$P_1 = P_2 e^{-i\omega t}, \quad (II-34)$$

$$T_1 = T_2 e^{-i\omega t}, \quad (II-35)$$

and

$$\bar{A} = \bar{A}_2 e^{-i\omega t}, \quad (II-36)$$

Then equations II-30, II-32, and II-33 are, after eliminating the numerical subscripts,

$$\eta_{st} \nabla^2 \bar{A} + i\omega \rho_{0t} \bar{A} = 0, \quad (II-37)$$

$$\left(1 - \frac{i\omega \xi}{\rho_{0t} c_1^2}\right) \nabla^2 P + \frac{\omega^2}{c_1^2} P = 0, \quad (II-38)$$

and

$$\nabla^2 P + \frac{\omega^2}{c_w^2} P = 0. \quad (II-39)$$

The coefficient of thermal expansion, β , is defined as

$$\beta = - \frac{1}{\rho_0} \left(\frac{\partial \rho_0}{\partial T} \right)_P, \quad (II-40)$$

so that, in air, equation II-14 is

$$\rho_{1a} = \frac{Y_a P_1}{c_a^2} - \rho_{0a} \beta_a T_1. \quad (II-41)$$

In addition, equations II-11 through II-13 for air are, after substitution for \bar{u} :

$$\frac{\partial \rho_{1a}}{\partial t} - \rho_{0a} \nabla^2 \Omega = 0, \quad (II-42)$$

$$\rho_{0a} \frac{\partial}{\partial t} (\nabla \times \bar{A}) = \rho_{0a} \frac{\partial}{\partial t} (\nabla \Omega) - \nabla P_1, \quad (II-43)$$

and

$$\rho_{0a} c_{va} \frac{\partial T_1}{\partial t} - \rho_{0a} \frac{(c_{pa} - c_{va})}{\beta_a} \nabla^2 \Omega - \kappa_a \nabla^2 T_1 = 0. \quad (II-44)$$

Taking the curl of equation II-43 and utilizing equation II-28 indicates that

$$\nabla \times \bar{A} = 0, \quad (II-45)$$

so that

$$\nabla P_1 - \rho_{0a} \frac{\partial}{\partial t} (\nabla \Omega) = 0. \quad (II-46)$$

Then, substitution of equation II-41 into II-42 yields:

$$\nabla^2 \Omega = \frac{\partial}{\partial t} \left[\frac{Y_a P_1}{\rho_{0a} c_a^2} - \beta_a T_1 \right]. \quad (II-47)$$

Hence, taking the divergence of equation II-46 and substitution of equation II-47 yields:

$$\nabla^2 P_1 - \rho_{0a} \frac{\partial^2}{\partial t^2} \left[\frac{Y_a P_1}{\rho_{0a} c_a^2} - \beta_a T_1 \right] = 0. \quad (II-48)$$

In addition, substitution of equation II-47 into II-44 yields:

$$\rho_{0a} c_{pa} \frac{\partial T_1}{\partial t} - \frac{Y_a (c_{pa} - c_{va})}{\beta_a c_a^2} \frac{\partial P_1}{\partial t} - \kappa_a \nabla^2 T_1 = 0. \quad (II-49)$$

Introduction of the harmonic time dependence into equations II-48 and II-49 yields, after eliminating the numerical subscripts:

$$\nabla^2 P + \frac{\omega^2 Y_a}{c_a^2} P - \omega^2 \rho_{0a} \beta_a T = 0 \quad (II-50)$$

and

$$\nabla^2 T + \frac{i\omega\rho_{0a}c_{pa}}{\kappa_a} T - \frac{i\omega Y_a(c_{pa} - c_{va})}{\beta_a c_a^2 \kappa_a} P = 0 \quad (II-51)$$

Equation II-50 can be written in terms of P alone by taking the Laplacian and substituting equations II-51 and II-50 for $\nabla^2 T$ and T, respectively, into the resulting equation. The result of this procedure is

$$\nabla^4 P + \left[\frac{\omega^2 Y_a}{c_a^2} + \frac{i\omega\rho_{0a}c_{pa}}{\kappa_a} \right] \nabla^2 P + \frac{i\omega^3\rho_{0a}c_{pa}}{\kappa_a c_a^2} P = 0 \quad (II-52)$$

Equation II-52 is reduced by considering it as a quadratic equation in ∇^2 . Then

$$(\nabla^2 + k_{1a}^2)(\nabla^2 + k_{2a}^2)P = 0 \quad (II-53)$$

where

$$2(k_{1a}^2 + k_{2a}^2) = \frac{\omega^2 Y_a}{c_a^2} + \frac{i\omega\rho_{0a}c_{pa}}{\kappa_a} \pm \frac{i\omega\rho_{0a}c_{pa}}{\kappa_a} \left[1 - \frac{\omega^2 \kappa_a^2 Y_a^2}{\rho_{0a}^2 c_a^4 c_{pa}^2} - \frac{2i\omega \kappa_a (Y_a - 2)}{\rho_{0a} c_a^2 c_{pa}} \right]^{1/2} \quad (II-54)$$

The second and third terms under the radical are much smaller than 1 for the ranges of parameters selected for this study, so that the radical can be approximated as

$$(1 - z)^{1/2} \approx 1 - \frac{z}{2} \quad (II-55)$$

Thus,

$$k_{1a}^2 = \frac{i\omega\rho_{0a}c_{pa}}{\kappa_a} + \frac{\omega^2(Y_a - 1)}{c_a^2} - \frac{i\omega^3 \kappa_a Y_a^2}{4\rho_{0a} c_a^4 c_{pa}} \quad (II-56)$$

and

$$k_{2a}^2 = \frac{\omega^2}{c_a^2} + \frac{i\omega^3 \kappa_a Y_a^2}{4\rho_{0a} c_a^4 c_{pa}} \quad (II-57)$$

An examination of the relative magnitudes of the terms in equations II-56 and II-57 shows that

$$k_{1a}^2 \approx \frac{i\omega\rho_{0a}c_{pa}}{\kappa_a} \quad (II-58)$$

or

$$k_{1a} \approx (1 + i) \left(\frac{\omega\rho_{0a}c_{pa}}{2\kappa_a} \right)^{1/2} \quad (II-59)$$

and

$$k_{2a} \approx \frac{\omega}{c_a} \quad (II-60)$$

Since k_{1a} and k_{2a} are never equal, the general solution of equation 11-53 is

$$P = \psi_1 + \psi_2, \quad (II-61)$$

where ψ_1 and ψ_2 satisfy the equations

$$(\nabla^2 + k_{1a}^2) \psi_1 = 0 \quad (II-62)$$

and

$$(\nabla^2 + k_{2a}^2) \psi_2 = 0. \quad (II-63)$$

Equations II-37 through II-39 can be written in a form similar to equations II-62 and II-63. Thus

$$(\nabla^2 + k_{3f}^2) \bar{A} = 0, \quad (II-64)$$

$$(\nabla^2 + k_{2f}^2) P = 0, \quad (II-65)$$

and

$$(\nabla^2 + k_{2w}^2) P = 0, \quad (II-66)$$

where

$$k_{3f}^2 = \frac{i\omega\rho_{0f}}{\eta_{sf}}, \quad (II-67)$$

$$k_{2f}^2 = \frac{\omega^2}{c_f^2} \left(1 - \frac{i\omega\xi}{\rho_{0f}c_f^2} \right)^{-1}, \quad (II-68)$$

and

$$k_{2w}^2 = \frac{\omega^2}{c_w^2}. \quad (II-69)$$

Comparisons of the equations for air and water indicate that ψ_2 represents a compressional wave. Hence, ψ_1 represents a thermal wave.

Equation II-64 can be transformed into a scalar equation. It can be shown that a vector $\bar{\Gamma}$ exists such that [48]

$$\bar{u} = \nabla^2 \bar{\Gamma} \quad (II-70)$$

and

$$\bar{A} = \nabla \times \bar{\Gamma}. \quad (II-71)$$

Since the problem is axisymmetric, $\partial/\partial\phi = 0$, which implies that $\Gamma_\phi = 0$. Thus

$$\nabla \times \bar{\Gamma} = \tilde{r}(0) + \tilde{\theta}(0) + \tilde{\phi} \frac{1}{r} \left[\frac{\partial}{\partial r}(r\Gamma_\theta) - \frac{\partial \Gamma_r}{\partial \theta} \right], \quad (II-72)$$

so that

$$\bar{A} = \tilde{\phi} A_\phi, \quad (II-73)$$

where \tilde{r} , $\tilde{\theta}$, and $\tilde{\phi}$ are unit vectors. Therefore

$$\nabla^2 \bar{A} = \tilde{\phi} \left[\nabla^2 A_\phi - \frac{A_\phi}{r^2 \sin^2 \theta} \right], \quad (II-74)$$

and equation II-64 can be written as

$$\nabla^2 A_p - \frac{A_p}{r^2 \sin^2 \theta} + k_{3f}^2 A_p = 0 \quad (II-75)$$

The plane wave impinging on the shell will be represented by

$$P_{wi} = A e^{ik_{2w}z} \quad (II-76)$$

where P_{wi} is the perturbation pressure of the wave in water, and A is the pressure amplitude. P_{wi} can be expanded in spherical waves as

$$P_{wi} = A \sum_{\ell=0}^{\infty} (2\ell + 1) i^{\ell} j_{\ell}(k_{2w}r) P_{\ell}(\cos \theta) \quad (II-77)$$

where ℓ is the mode number, $j_{\ell}(k_{2w}r)$ is a spherical Bessel function and $P_{\ell}(\cos \theta)$ is a Legendre polynomial. The incidence of the wave upon the shell gives rise to five additional waves, which are represented by the solutions of equations II-62, II-63, II-65, II-66, and II-75. These equations can be solved by standard separation of variables techniques. The solutions are:

$$\psi_1 = \sum_{\ell=0}^{\infty} D_{a\ell} j_{\ell}(k_{1a}r) P_{\ell}(\cos \theta) \quad (II-78)$$

$$\psi_2 = \sum_{\ell=0}^{\infty} B_{a\ell} j_{\ell}(k_{2a}r) P_{\ell}(\cos \theta) \quad (II-79)$$

$$P_f = \sum_{\ell=0}^{\infty} [B_{f\ell} j_{\ell}(k_{2f}r) + E_{f\ell} n_{\ell}(k_{2f}r)] P_{\ell}(\cos \theta) \quad (II-80)$$

$$P_{ws} = \sum_{\ell=0}^{\infty} B_{w\ell} h_{\ell}(k_{2w}r) P_{\ell}(\cos \theta) \quad (II-81)$$

and

$$A_{\phi f} = \sum_{\ell=1}^{\infty} [F_{f\ell} j_{\ell}(k_{3f}r) + G_{f\ell} n_{\ell}(k_{3f}r)] P'_{\ell}(\cos \theta) \quad (II-82)$$

where B , D , E , F , and G represent the amplitudes of the waves, $\eta_{\ell}(k_{2f}r)$ is a spherical Neumann function, and $h_{\ell}(k_{2w}r)$ is a spherical Hankel function of the first kind. P_{ws} indicates the scattered compressional wave in water, so that

$$P_w = P_{wi} + P_{ws} \quad (II-83)$$

One of the assumptions of this model is that only the fundamental mode contributes to the scattering. Thus only the $\ell = 0$ mode is considered. Examination of equation II-82 shows that for $\ell = 0$,

$$A_{\phi f} = 0 \quad (II-84)$$

The remaining equations are now written for $\ell = 0$:

$$P_w = A j_0(k_{2w}r) + B_w h_0(k_{2w}r) \quad (II-85)$$

$$P_f = B_{f0}(k_{2f}r) + E_{f0}(k_{2f}r) \quad (II-86)$$

$$\psi_1 = D_{a0}(k_{1a}r) \quad (II-87)$$

and

$$\psi_2 = B_{aj_0}(k_{2a}r) , \quad (II-88)$$

where the numerical subscripts have been eliminated from the coefficients for convenience.

The scattering cross section of the shell is

$$\sigma = \Phi_s / I_i , \quad (II-89)$$

where Φ_s is the average scattered power and I_i the incident intensity.

$$\Phi_s = \frac{1}{2} \int_{\vec{r} \rightarrow \infty} P_{ws}^* u_{rws} d\vec{v} , \quad (II-90)$$

where \vec{v} is the area of an element of a sphere [49].

$$\vec{v} = \bar{n} v , \quad (II-91)$$

$$dv = r^2 d\chi , \quad (II-92)$$

where \bar{n} is the normal to the area and χ is the solid angle. Also,

$$I_i = \frac{1}{2} P_{wi}^* u_{wi} \quad (II-93)$$

so that it is necessary to determine u_{rws} and u_{wi} in terms of P_{ws} and P_{wi} , respectively [49].

In the fundamental mode $\bar{u} = -\nabla\Omega$, so that utilizing equation II-31 for water,

$$P_w - \rho_{0w} \frac{\partial \Omega}{\partial t} = 0 . \quad (II-94)$$

Introducing the harmonic time dependence yields:

$$\Omega_w = \frac{i}{\omega \rho_{0w}} P_w , \quad (II-95)$$

so that

$$u_{rws} = -\frac{i}{\omega \rho_{0w}} \frac{\partial P_{ws}}{\partial r} \quad (II-96)$$

and

$$u_{wi} = -\frac{i}{\omega \rho_{0w}} \frac{\partial P_{wi}}{\partial z} . \quad (II-97)$$

Thus, from equations II-76 and II-97,

$$I_i = \frac{A^2}{2\rho_{0w}c_w} . \quad (II-98)$$

From equation II-81,

$$P_{ws} = B_w h_0(k_{2w}r) , \quad (II-99)$$

where

$$h_0(k_{2w}r) = \frac{e^{ik_{2w}r}}{ik_{2w}r} , \quad (II-100)$$

so that for $r \rightarrow \infty$,

$$h_0'(k_{2w}r) = \frac{e^{ik_{2w}r}}{r}, \quad (II-101)$$

Thus, as $r \rightarrow \infty$,

$$P_{ws}^* u_{rws} = \frac{B_w B_w^*}{\omega \rho_{0w} k_{2w}} \quad (II-102)$$

and

$$\Phi_s = \frac{2\pi B_w B_w^*}{\omega \rho_{0w} k_{2w}}. \quad (II-103)$$

Therefore,

$$\sigma = \frac{4\pi |B_w|^2}{k_{2w}^2 A^2}, \quad (II-104)$$

and in order to determine σ , it is necessary to solve equations II-85 through II-88 for (B_w/A) .

Boundary Conditions

Equations II-85 through II-88 contain five unknown coefficients. Thus, five boundary conditions are required for the solution of this set of equations. These conditions are the continuity of normal velocity, u_r , and normal stress, τ_{rr} , at both interfaces and continuity of temperature at the inner interface. The first step in solving for B_w/A , therefore, is to obtain u_r , τ_{rr} and T in terms of P_w , P_r , ψ , and ψ_2 .

Equation II-50 gives T_a in terms of P_a . Substitution of equations II-58 and II-60 through II-63 into equation II-50 leads to

$$T_a = \frac{1}{\rho_{0a} c_a^2 \beta_a} \left\{ \left[\gamma_a - \frac{i \rho_{0a} c_a^2 c_{pa}}{\omega K_a} \right] \psi_1 + (\gamma_a - 1) \psi_2 \right\}. \quad (II-105)$$

u_{rw} is given in terms of P_w by equation II-96. Following the same procedure to obtain u_{rr} , equation II-31 may be written as

$$P_r + \xi \nabla^2 \Omega_r - \rho_{0r} \frac{\partial \Omega_r}{\partial t} = 0. \quad (II-106)$$

Then substitution of equation II-26 into II-106 yields, with introduction of the harmonic time dependence:

$$\Omega_r = \frac{i}{\omega \rho_{0r}} \left[1 - \frac{i \omega \xi}{\rho_{0r} c_r^2} \right] P_r. \quad (II-107)$$

Similarly, from equation II-46 and II-61:

$$\Omega_a = \frac{i}{\omega \rho_{0a}} (\psi_1 + \psi_2). \quad (II-108)$$

Thus,

$$u_{rr} = -\frac{i}{\omega \rho_{0r}} \left[1 - \frac{i \omega \xi}{\rho_{0r} c_r^2} \right] \frac{\partial P_r}{\partial r} \quad (II-109)$$

and

$$u_{ra} = -\frac{i}{\omega \rho_{0a}} \left[\frac{\partial \psi_1}{\partial r} + \frac{\partial \psi_2}{\partial r} \right]. \quad (II-110)$$

The normal stress in fish flesh is [45]

$$\tau_{rrf} = -P_f + \xi \frac{\partial u_r}{\partial r}, \quad (II-111)$$

so that utilization of equation II-109 yields:

$$\tau_{rrf} = -P_f - \frac{i\xi}{\omega\rho_{0f}} \left[1 - \frac{i\omega\xi}{\rho_{0f}c_f^2} \right] \frac{\partial^2 P_f}{\partial r^2}. \quad (II-112)$$

Also,

$$\tau_{rrw} = -P_w. \quad (II-113)$$

and

$$\tau_{rra} = -P_a. \quad (II-114)$$

At the air fish-flesh interface the surface tension must be included in the stress equation. For a bubble in water [50],

$$P_{in} = P_{out} + \frac{2s}{R}, \quad (II-115)$$

where P_{in} and P_{out} are the total pressures inside and outside the bubble and R is the radius of the bubble at any instant. If g represents the small changes in the radius of the bubble and a is the average radius, such that

$$R = a + g, \quad (II-116)$$

where $g \ll a$, then

$$\frac{2}{R} = \frac{2}{a(1 + g/a)} \approx \frac{2}{a} (1 - g/a), \quad (II-117)$$

so that

$$P_{in} = P_{out} + \frac{2s}{a} (1 - g/a). \quad (II-118)$$

Since P_{in} and P_{out} are total pressures, equation II-118 can be linearized utilizing equation II-10. Thus, the first order equation is

$$P_{out1} = P_{in1} + \frac{2sg}{a^2}. \quad (II-119)$$

Due to the harmonic time dependence,

$$u_r = \frac{\partial R}{\partial t} = -i\omega g. \quad (II-120)$$

Thus

$$P_{out1} - P_{in1} = \frac{2is u_{r0}}{\omega a^2}. \quad (II-121)$$

The boundary conditions are:

$$\text{BC 1} \quad u_{rw} = u_{rf} \quad \text{at} \quad r = b, \quad (II-122)$$

$$\text{BC 2} \quad \tau_{rrw} = \tau_{rrf} \quad \text{at} \quad r = b, \quad (II-123)$$

$$\text{BC 3} \quad u_{rf} = u_{ra} \quad \text{at} \quad r = a, \quad (\text{II-124})$$

$$\text{BC 4} \quad \tau_{rf} = \tau_{ra} - \frac{2iu_{ra}s}{\omega a^2} \quad \text{at} \quad r = a, \quad (\text{II-125})$$

$$\text{BC 5} \quad T_a = 0 \quad \text{at} \quad r = a. \quad (\text{II-126})$$

Equations II-122 through II-126 have been labeled BC 1 through BC 5 for later convenience. Substitution of equations II-105, II-109, II-110, II-96, II-112, II-113, II-114, and II-85 through II-88 into equations II-122 through II-126 yields:

$$\begin{aligned} \text{BC 1,} \quad & \left(\frac{1}{\rho_{0w}} \right) \left[A k_{2w} j_0'(k_{2w} b) + B_w k_{2w} h_0'(k_{2w} b) \right] \\ & = \left(\frac{1}{\rho_{0f}} \right) \left(1 - \frac{i\omega\xi}{\rho_{0f} c_f^2} \right) \left[B_f k_{2f} j_0'(k_{2f} b) + E_f k_{2f} n_0'(k_{2f} b) \right]; \end{aligned} \quad (\text{II-127})$$

$$\begin{aligned} \text{BC 2,} \quad & A j_0(k_{2w} b) + B_w h_0(k_{2w} b) = B_{f0}(k_{2f} b) + E_f n_0(k_{2f} b) \\ & + \left(\frac{i\xi}{\omega \rho_{0f}} \right) \left(1 - \frac{i\omega\xi}{\rho_{0f} c_f^2} \right) \left[B_f k_{2f}^2 j_0''(k_{2f} b) + E_f k_{2f}^2 n_0''(k_{2f} b) \right]; \end{aligned} \quad (\text{II-128})$$

$$\begin{aligned} \text{BC 3,} \quad & \left(\frac{1}{\rho_{0f}} \right) \left(1 - \frac{i\omega\xi}{\rho_{0f} c_f^2} \right) \left[B_f k_{2f} j_0'(k_{2f} a) + E_f k_{2f} n_0'(k_{2f} a) \right] \\ & = \left(\frac{1}{\rho_{0a}} \right) \left[D_a k_{1a} j_0'(k_{1a} a) + B_a k_{2a} j_0'(k_{2a} a) \right]; \end{aligned} \quad (\text{II-129})$$

$$\begin{aligned} \text{BC 4,} \quad & B_{f0}(k_{2f} a) + E_f n_0(k_{2f} a) + \left(\frac{i\xi}{\omega \rho_{0f}} \right) \left(1 - \frac{i\omega\xi}{\rho_{0f} c_f^2} \right) \left[B_f k_{2f}^2 j_0''(k_{2f} a) + E_f k_{2f}^2 n_0''(k_{2f} a) \right] \\ & = D_{aj0}(k_{1a} a) + B_{aj0}(k_{2a} a) + \left(\frac{2s}{\omega^2 a^2 \rho_{0a}} \right) \left[D_a k_{1a} j_0'(k_{1a} a) + B_a k_{2a} j_0'(k_{2a} a) \right]; \end{aligned} \quad (\text{II-130})$$

$$\text{and BC 5,} \quad \left(\gamma_a - \frac{i\rho_{0a} c_{pa} c_a^2}{\omega \kappa_a} \right) D_{aj0}(k_{1a} a) + (\gamma_a - 1) B_{aj0}(k_{2a} a) = 0. \quad (\text{II-131})$$

CHAPTER III

SOLUTION

The first step in the solution of equations II-127 through II-131 for (B_w/A) is to solve II-131 for D_a and substitute the result into equations II-129 and II-130. For conciseness the boundary conditions will now be written in a tabular form:

BC	B_w	B_f	E_f	B_a	A
1	S_{11}	S_{12}	S_{13}	0	α_1
2	S_{21}	S_{22}	S_{23}	0	α_2
3	0	S_{32}	S_{33}	S_{34}	0
4	0	S_{42}	S_{43}	S_{44}	0

The S_{ij} 's are taken such that

$$S_{11}B_w + S_{12}B_f + S_{13}E_f + S_{14}B_a = \alpha_1 A \quad (\text{III-1})$$

The S_{ij} 's and α 's are as follows:

$$S_{11} = -\left(\frac{k_{2w}}{\rho_{0w}}\right) h_0'(k_{2w}b) , \quad (\text{III-2})$$

$$S_{12} = \left(\frac{\omega^2}{\rho_{0f}c_f^2k_{2f}}\right) j_0'(k_{2f}b) , \quad (\text{III-3})$$

$$S_{13} = \left(\frac{\omega^2}{\rho_{0f}c_f^2k_{2f}}\right) n_0'(k_{2f}b) \quad (\text{III-4})$$

$$\alpha_1 = \left(\frac{k_{2w}}{\rho_{0w}}\right) j_0(k_{2w}b) , \quad (\text{III-5})$$

$$S_{21} = -h_0(k_{2w}b) , \quad (\text{III-6})$$

$$S_{22} = j_0(k_{2f}b) + \left(\frac{i\omega\xi}{\rho_{0f}c_f^2}\right) j_0''(k_{2f}b) , \quad (\text{III-7})$$

$$S_{23} = n_0(k_{2f}b) + \left(\frac{i\omega\xi}{\rho_{0f}c_f^2}\right) n_0''(k_{2f}b) , \quad (\text{III-8})$$

$$\alpha_2 = j_0(k_{2w}b) , \quad (\text{III-9})$$

$$S_{32} = \left(\frac{\omega^2}{\rho_{0f}c_f^2k_{2f}}\right) j_0'(k_{2f}a) , \quad (\text{III-10})$$

$$S_{33} = \left(\frac{\omega^2}{\rho_{0f}c_f^2k_{2f}}\right) n_0'(k_{2f}a) , \quad (\text{III-11})$$

$$S_{34} = \left(\frac{1}{\rho_{0a}}\right) \left[\frac{(\gamma_a - 1) k_{1a} j_0'(k_{1a}a) j_0(k_{2a}a)}{\left(\gamma_a - \frac{i\rho_{0a}c_{pa}c_a^2}{\omega\kappa_a}\right) j_0(k_{1a}a)} - k_{2a} j_0'(k_{2a}a) \right] , \quad (\text{III-12})$$

$$S_{42} = j_0(k_{2f}a) + \left(\frac{i\omega\xi}{\rho_{0f}c_f^2}\right) j_0''(k_{2f}a) , \quad (\text{III-13})$$

$$S_{43} = n_0(k_{2f}a) + \left(\frac{i\omega\xi}{\rho_{0f}c_f^2}\right) n_0''(k_{2f}a) , \quad (\text{III-14})$$

$$S_{44} = \left[\frac{(\gamma_a - 1)j_0(k_{2a}a)}{\left(\gamma_a - \frac{i\rho_{0a}c_a^2 c_{pa}}{\omega \kappa_a} \right)} \right] \left[1 + \left(\frac{2s}{\omega^2 a^2 \rho_{0a}} \right) \left(\frac{k_{1a} j_0'(k_{1a}a)}{j_0(k_{1a}a)} \right) \right] + j_0(k_{2a}a) + \left(\frac{2s\kappa_a}{\omega^2 a^2 \rho_{0a}} \right) j_0'(k_{2a}a) , \quad (III-15)$$

where equation II-68 has been used for k_{21}^2 .

The solution of the boundary conditions for B_w is

$$\frac{B_w}{A} = \frac{\alpha_1 U + \alpha_2 W}{S_{11}U + S_{21}W} \quad (III-16)$$

where

$$U = S_{44}(S_{22}S_{33} - S_{23}S_{32}) + S_{34}(S_{23}S_{42} - S_{22}S_{43}) \quad (III-17)$$

and

$$W = S_{44}(S_{13}S_{32} - S_{12}S_{33}) + S_{34}(S_{12}S_{43} - S_{13}S_{42}) . \quad (III-18)$$

This solution is easily arrived at after several pages of substitutions.

Equation III-16 could be solved numerically with a computer by choosing values for the various physical parameters and calculating the S_{ij} 's and α_i 's. However, this will not be done because the purpose of this report is to obtain simplified equations for ω_0 and σ which can be solved without resorting to use of a computer. The simplified solution is based on the ranges of the physical properties and the limits of the variables given in Chapter II. It is obtained by assuming that $|k_{1a}a|$ is large and that $k_{2w}b$, $k_{21}b$, and $k_{2a}a$ are small and accepting any errors which are less than ten percent. Order of magnitude comparisons are then made between various terms and any term which is always less than ten percent of another term is neglected. This simplification process is shown in Appendix B. The result of this process is:

$$\frac{B_w}{A} = - (1 + \Lambda + i\lambda) \left\{ 1 + \frac{2\xi c_w}{\rho_{0w}\omega^2 a^3} + \left[\frac{3\rho_{0f}c_w(\gamma_a - 1)}{\rho_{0w}\omega^2 a^2} \right] \left(\frac{\omega \kappa_a}{2\rho_{0a}c_{pa}} \right)^{1/2} \left(1 + \frac{2s}{\omega^2 a^3 \rho_{0f}} \right) + i \left(\frac{c_w \rho_{0f}}{\omega a \rho_{0w}} \right) \left[\left(\frac{3\rho_{0a}c_a^2}{\omega^2 a^2 \rho_{0f}} \right) \left(1 - \frac{2s}{3\rho_{0a}c_a^2 a} \right) - 1 - \left(\frac{11\xi^2}{3\rho_{0f}^2 c_f^2 a^2} \right) \right] \right\}^{-1} , \quad (III-19)$$

where

$$\Lambda = \left(\frac{\omega^2 \xi^2 b^3}{\rho_{0f}^2 c_f^4 a^3} \right) \left(\frac{11\rho_{0f}c_f^2}{9\rho_{0w}c_w^2} - 1 \right) \quad (III-20)$$

and

$$\lambda = \left(\frac{2\omega \xi b^3}{3\rho_{0f}c_f^2 a^3} \right) \left[\left(\frac{\rho_{0f}c_f^2}{\rho_{0w}c_w^2} - 1 \right) - \left(\frac{\rho_{0f}c_f^2}{\rho_{0w}c_w^2} + \frac{11}{4} \right) \left(\frac{a^3}{b^3} \right) \right] . \quad (III-21)$$

Equation III-19 can now be substituted into II-104 to yield σ . However, before doing this, equation III-19 will be manipulated so that the final results can be easily compared to those of other researchers. Thus, the resonant frequency is determined by setting the imaginary part of the denominator of equation III-19 equal to zero and the real terms of the denominator represent the damping [18]. Therefore, letting

$$\left(\frac{3\rho_{0a}c_a^2}{\omega^2 a^2 \rho_{0f}} \right) \left(1 - \frac{2s}{3\rho_{0a}c_a^2 a} \right) - 1 - \left(\frac{11\xi^2}{3\rho_{0f}c_f^2 a^2} \right) = 0 \quad (\text{III-22})$$

and solving for $\omega^2 a^2$ yields the resonant frequency of the new model:

$$\omega_0^2 a^2 = \frac{\frac{3\rho_{0a}c_a^2}{\rho_{0f}} \left(1 - \frac{2s}{3\rho_{0a}c_a^2 a} \right)}{\left(1 + \frac{11\xi^2}{3\rho_{0f}^2 c_f^2 a^2} \right)} \quad (\text{III-23})$$

Now [42],

$$\rho_{0a}c_a^2 = \gamma_a P_{0a} \quad (\text{III-24})$$

and from equation II-115,

$$P_{0a} = P_{0f} + \frac{2s}{a} = P_{0w} + \frac{2s}{a} \quad (\text{III-25})$$

Therefore, substitution of equations III-24 and III-25 into III-23 yields:

$$\omega_0^2 a^2 = \frac{\frac{3\gamma_a P_{0w}}{\rho_{0f}} + \frac{2s}{\rho_{0f} a} (3\gamma_a - 1)}{\left(1 + \frac{11\xi^2}{3\rho_{0f}^2 c_f^2 a^2} \right)} \quad (\text{III-26})$$

The damping factor, H, will be defined by

$$\frac{\omega_0}{\omega H} = \frac{\rho_{0w} \omega a}{\rho_{0f} c_w} + \frac{2\xi}{\rho_{0f} \omega a^2} + \frac{3(\gamma_a - 1)}{\omega a} \left(\frac{\omega \kappa_a}{2\rho_{0a} c_{pa}} \right)^{1/2} \left(1 + \frac{2s}{\rho_{0f} \omega^2 a^3} \right) \quad (\text{III-27})$$

Thus, following Devin [19],

$$\frac{1}{H} = \frac{1}{H_{rad}} + \frac{1}{H_{vis}} + \frac{1}{H_{th}} = d \quad (\text{III-28})$$

where

$$H_{rad} = \frac{\omega_0 \rho_{0f} c_w}{\omega^2 \rho_{0w} a} \quad (\text{III-29})$$

$$H_{vis} = \frac{\omega_0 \rho_{0f} a^2}{2\xi} \quad (\text{III-30})$$

and

$$H_{th} = \frac{\omega_0 a}{3(\gamma_a - 1)} \left(\frac{2\rho_{0a} c_{pa}}{\omega \kappa_a} \right)^{1/2} \left(1 + \frac{2s}{\rho_{0f} \omega^2 a^3} \right)^{-1} \quad (\text{III-31})$$

As before, at $\omega = \omega_0$, $H = Q$. Thus, substitution of equations III-26 and III-27 into III-19 yields:

$$\frac{B_w}{A} = \frac{-\left(\frac{\rho_{0w}\omega a}{\rho_{0f}c_w}\right) (1 + \Lambda + i\lambda)}{\left(\frac{\omega_0}{\omega H}\right) + i\left(\frac{\omega_0^2}{\omega^2} - 1\right) \left(1 + \frac{11\xi^2}{3\rho_{0f}c_f^2a^2}\right)} \quad (\text{III-32})$$

Then, substitution of equation III-32 into II-104 yields the scattering cross section of the new model:

$$\sigma = \frac{4\pi a^2 \left(\frac{\rho_{0w}}{\rho_{0f}}\right)^2 [(1 + \Lambda)^2 + \lambda^2]}{\left(\frac{\omega_0^2}{\omega^2 H^2}\right) + \left(\frac{\omega_0^2}{\omega^2} - 1\right)^2 \left(1 + \frac{11\xi^2}{3\rho_{0f}^2 c_f^2 a^2}\right)^2} \quad (\text{III-33})$$

where Λ , λ , ω_0 , and H are given in equations III-20, III-21, III-26, and III-27.

CHAPTER IV

DISCUSSION

Results

The equations developed for ω_0 , σ , and H in Chapter III for the new model can be considered to be accurate within ten percent only for the parameter ranges given in Chapter II. The ranges of ξ , for which exact values are not known, and s , which may be varied, were extended beyond the limits of present available data. However, the largest values of a , ω , and P_{0w} used in this model are not beyond the range of possible values. These limitations were imposed by the assumption that $k_{2a}a$ is small. This required that, for the error caused by using just the first term of the spherical Bessel function expansions to be less than ten percent,

$$\omega a < 2.4 \times 10^4 \text{ cm/sec.}$$

The limitation of $k_{2a}a$ being small is a factor in all the previous models, but in most cases it is not mentioned or, if it is mentioned, no limiting value is given.

The range of ξ utilized in the solution of the new model was

$$1 \text{ poise} \leq \xi \leq 10^4 \text{ poise.}$$

However, a more likely range of ξ , as shown in Appendix A, is

$$50 \text{ poise} \leq \xi \leq 2 \times 10^3 \text{ poise.}$$

This narrower range will be utilized in the remainder of the discussion because it results in a simplification of equations III-26 and III-34 without, in all probability, affecting the results. Equations III-26 and III-34 simplify to

$$\omega_0^2 a^2 = \frac{3\gamma_a P_{0w}}{\rho_{0f}} + \frac{2s}{\rho_{0f} a} (3\gamma_a - 1) \quad (\text{IV-1})$$

and

$$\sigma = \frac{4\pi a^2 \left(\frac{\rho_{0w}}{\rho_{0f}} \right)^2}{\left[\frac{\omega_0^2}{\omega^2 H^2} + \left(\frac{\omega_0^2}{\omega^2} - 1 \right)^2 \right]} \quad (\text{IV-2})$$

respectively, when the upper limit of ξ is reduced to 2×10^3 poise. Λ and λ are negligible compared to 1 for $\xi \leq 2 \times 10^3$ poise. Λ and λ were the only remaining terms which contained b . Thus, for the a/b range given in Chapter II, b is unimportant for $\xi \leq 2 \times 10^3$ poise.

Figure 2 gives $\omega_0 a$ as a function of depth and surface tension, calculated from equation IV-1. s has essentially no effect on $\omega_0 a$ for $s/a \leq 10^5$ dyne/cm² at any depth and for $s/a \leq 10^6$ dyne/cm² for depths below 100 m. For s/a values around 5×10^7 dyne/cm², pressure has essentially no effect on $\omega_0 a$ for depths less than 100 m and at a depth of 1000 m, $\omega_0 a$ is increased by only 50 percent over its value near the surface.

At resonance,

$$\sigma = 4\pi a^2 Q^2 \left(\frac{\rho_{0w}}{\rho_{0f}} \right)^2 \quad (\text{IV-3})$$

and

$$Q_{\text{rad}} = \frac{\rho_{0f} c_w}{\rho_{0w} \omega_0 a} \quad (\text{IV-4})$$

$$Q_{\text{vis}} = \frac{\omega_0 \rho_{0f} a^2}{2\xi} \quad (\text{IV-5})$$

and

$$Q_{\text{th}} = \frac{\omega_0^{1/2} a}{3(\gamma_a - 1)} \left(\frac{2\rho_{0a} c_{pa}}{\kappa_a} \right)^{1/2} \left(1 + \frac{2s}{\rho_{0f} \omega_0^2 a^3} \right)^{-1} \quad (\text{IV-6})$$

Thus, σ is proportional to Q^2 at resonance.

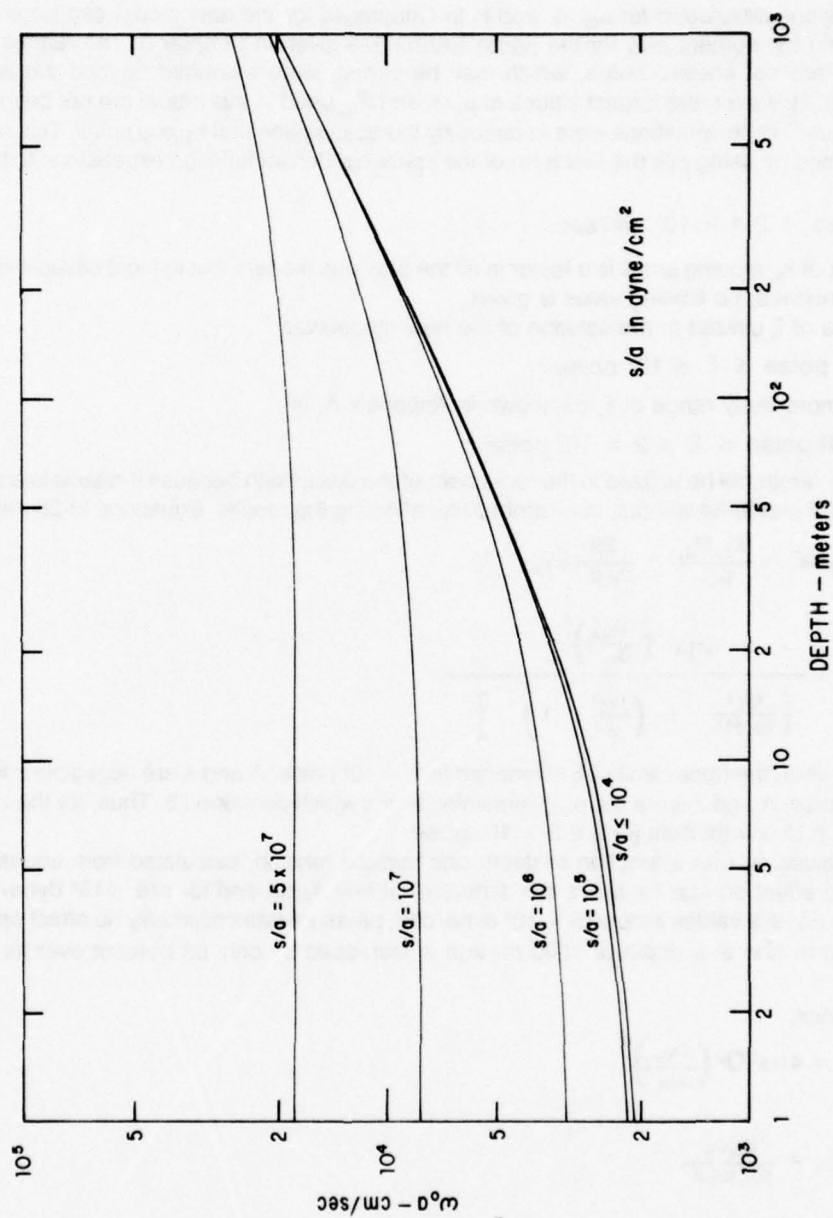


FIGURE 2. RESONANT FREQUENCY OF THE NEW MODEL OF A SWIMBLADDER-BEARING FISH

Figure 3 shows Q_{rad} and Q_{vis} as functions of $\omega_0 a$. Q_{vis} increases with increasing $\omega_0 a$ and decreases with increasing ξ/a . Values of

$$2 \times 10^2 \text{ poise/cm} \leq \xi/a \leq 10^3 \text{ poise/cm}$$

give values of Q_{vis} which are comparable to values obtained for Q in near-surface swimbladder resonance experiments [15, 33, 36-38]. Q_{rad} decreases with increasing $\omega_0 a$ and, depending upon the value of ξ/a , may be significant for all $\omega_0 a$ considered.

Figure 4 shows Q_{th} as a function of $\omega_0 a$, a , s/a , and depth D . Any individual numbered curve indicates that Q_{th} increases gradually with increasing s/a . The set of numbered curves indicates that Q_{th} increases with increasing a and D . The lettered curves are for the case where the effect of surface tension is insignificant, and also indicate that Q_{th} increases with increasing a and D . A comparison of figures 3 and 4 shows that Q_{th} is significant only at depths above 100 m and then only if $\xi/a < 10^3$ poise/cm.

At off-resonance frequencies

$$H_{rad} = \left(\frac{\omega_0}{\omega} \right)^2 Q_{rad} \quad , \quad (IV-7)$$

$$\text{and} \quad H_{vis} = Q_{vis} \quad , \quad (IV-8)$$

$$H_{th} = \left(\frac{\omega_0}{\omega} \right)^{1/2} \left[\frac{1 + \frac{2s}{\rho_{0f} \omega_0^2 a^3}}{1 + \frac{2s}{\rho_{0f} \omega^2 a^3}} \right] Q_{th} \quad . \quad (IV-9)$$

Thus, at frequencies above resonance, H_{rad} may be the dominant damping term, even for relatively high values of ξ/a . Conversely, at frequencies below resonance, H_{rad} may be the least important damping term. The variation of H_{th} with (ω_0/ω) is complicated by the presence of the surface tension term. It can be shown, utilizing equation IV-1, that

$$1 \leq 1 + \frac{2s}{\rho_{0f} \omega_0^2 a^3} \leq 1.31 \quad , \quad (IV-10)$$

so that, for the purpose of establishing a trend,

$$H_{th} \approx \left(\frac{\omega_0}{\omega} \right)^{1/2} \left(1 + \frac{2s}{\rho_{0f} \omega^2 a^3} \right)^{-1} Q_{th} \quad . \quad (IV-11)$$

Hence, at frequencies above resonance and at frequencies below resonance for which $\rho_{0f} \omega^2 a^3 \gg (2s/a)$,

$$H_{th} \approx \left(\frac{\omega_0}{\omega} \right)^{1/2} Q_{th} \quad . \quad (IV-12)$$

At frequencies below resonance for which $(2s/a) \gg \rho_{0f} \omega^2 a^3$,

$$H_{th} \approx \left(\frac{\omega_0}{\omega} \right)^{1/2} \left(\frac{\rho_{0f} \omega^2 a^3}{2s} \right) Q_{th} \quad . \quad (IV-13)$$

Thus, H_{th} becomes relatively less important than H_{rad} as frequency increases and conversely.

Comparison to Free Bubble

The validity of the results developed for the new model must be determined. This will be done by first checking that the equations developed for the new model approach the equations for a free bubble in water as a limiting case and then comparing values calculated using the new model with experimental values.

The equations obtained in Chapter III for the resonant frequency and scattering cross section of the new model can be readily compared to the equations given for a free bubble. Equations I-6 and I-7 give ω_0 and σ for an ideal bubble, neglecting surface tension. Equation III-26 reduces exactly to equation I-6 when $\xi = s = 0$. If thermal losses are also neglected, equation III-33 reduces to equation I-7 when $\xi = s = 0$, except for factors of (ρ_{0w}/ρ_{0f}) . If surface tension is included, ω_0 for an ideal bubble is given by equation I-12 with $\eta_{sw} = 0$. Equation III-26 reduces exactly to equation I-12 when $\xi = \eta_{sw} = 0$. Thus, when viscous and thermal dissipation effects are eliminated from the new model, the results are equivalent to results obtained for an ideal bubble.

When the viscosity of water is considered for an air bubble in water, ω_0 is given by equation I-12. A comparison of equation III-26 with I-12 shows that the form of the viscosity factor for the new model differs from that given for a bubble. However, as was noted earlier, equation I-12 is only valid for small viscosities, so that this difference is not surprising [25]. Both equations I-12 and III-26 indicate that ω_0 decreases as the viscosity increases, which should be the case for a viscously damped system [51].

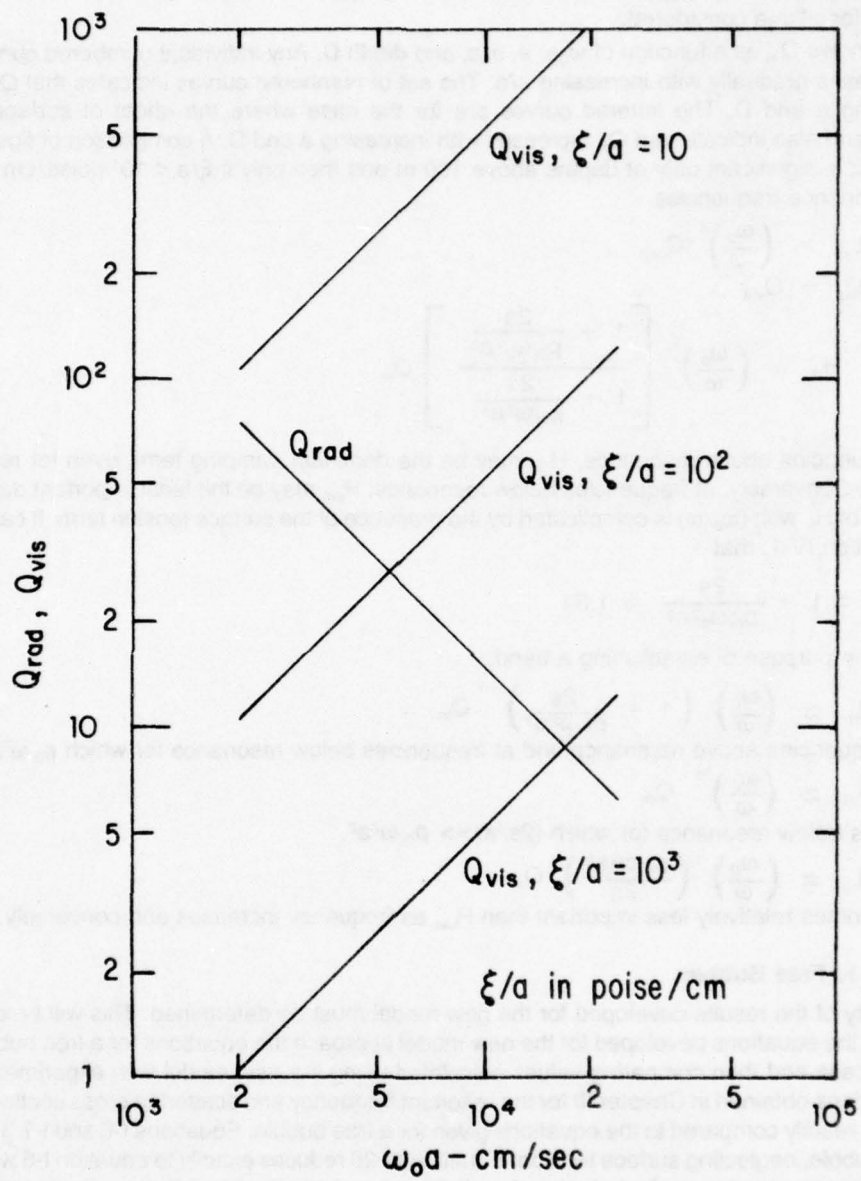


FIGURE 3. VISCOUS AND RADIATION DAMPING FACTORS FOR THE NEW MODEL OF A SWIMBLADDER-BEARING FISH

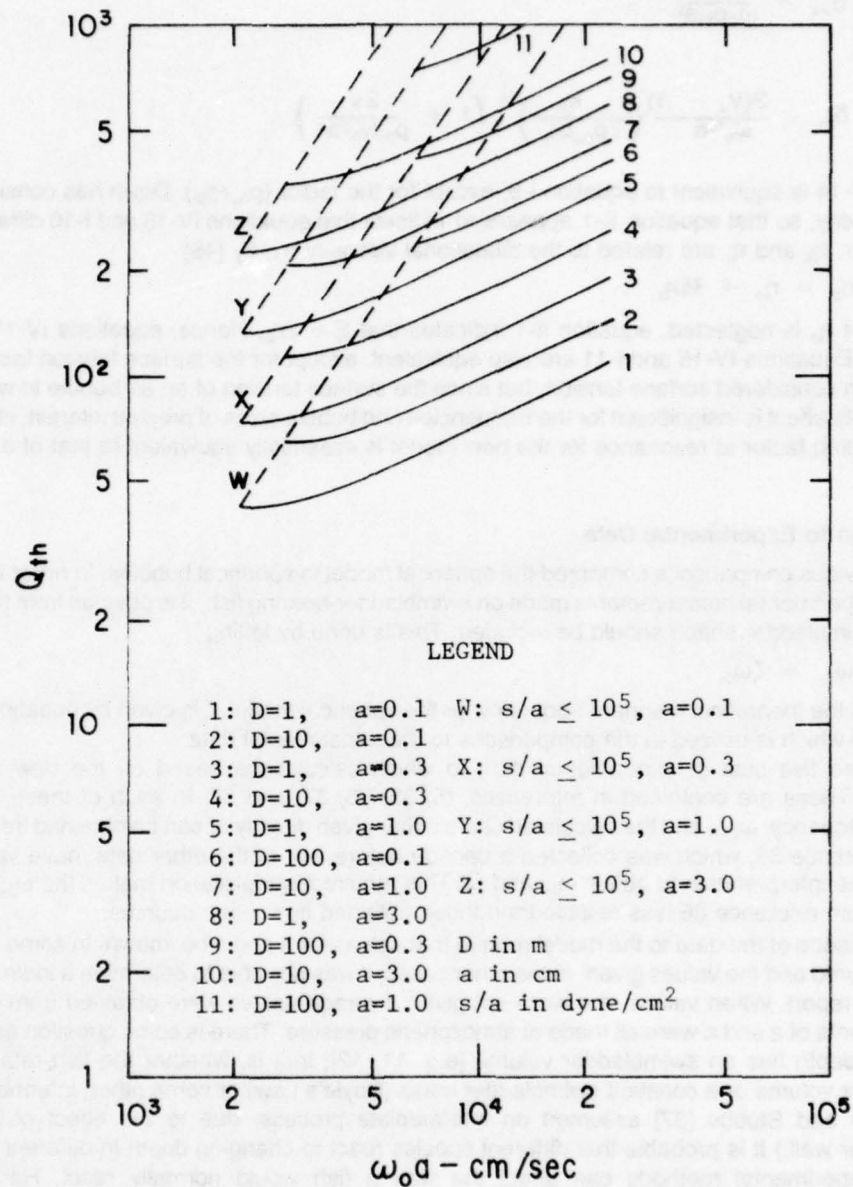


FIGURE 4. THERMAL DAMPING FACTORS FOR THE NEW MODEL OF A SWIMBLADDER-BEARING FISH

The damping in the new model can also be compared to that for a real bubble in water as determined by Devin [19]. For ease in comparison with Devin's results, equations IV-4, IV-5, and IV-6 will be rewritten as:

$$\delta_{\text{rad}} = \frac{\rho_{0w} \omega_0 a}{\rho_{0l} c_w} \quad , \quad (\text{IV-14})$$

$$\delta_{\text{vis}} = \frac{2\xi}{\omega_0 \rho_{0l} a^2} \quad , \quad (\text{IV-15})$$

and

$$\delta_{\text{th}} = \frac{3(\gamma_a - 1)}{\omega_0^{1/2} a} \left(\frac{\kappa_a}{2\rho_{0a} c_{pa}} \right)^{1/2} \left(1 + \frac{2s}{\rho_{0l} \omega_0^2 a^3} \right) \quad . \quad (\text{IV-16})$$

Equation IV-14 is equivalent to equation I-9, except for the factor (ρ_{0w}/ρ_{0l}) . Devin has considered only the shear viscosity, so that equation II-1 appears to indicate that equations IV-15 and I-10 differ by a factor of $2/3$. However, η_b and η_s are related to the dilatational viscosity η_d , by [45]

$$\eta_b = \eta_d + \frac{2}{3}\eta_s \quad . \quad (\text{IV-17})$$

Therefore, if η_d is neglected, equation II-1 indicates that $\xi = 2\eta_s$. Hence, equations IV-15 and I-10 are equivalent. Equations IV-16 and I-11 are also equivalent, except for the surface tension factor in equation IV-16. Devin considered surface tension, but since the surface tension of an air bubble in water is only 74 dynes/cm, its effect is insignificant for the frequencies and bubble sizes of present interest. Hence, the form of the damping factor at resonance for the new model is essentially equivalent to that of a real bubble in water.

Comparison to Experimental Data

The previous comparisons compared the spherical model to spherical bubbles. In order to compare the model to experimental measurements made on swimbladder-bearing fish, it is obvious from figure 1 that the effect of swimbladder shape should be included. This is done by letting

$$\omega_{0c} = \zeta \omega_{0l} \quad , \quad (\text{IV-18})$$

where ω_{0l} is the theoretical resonant frequency for the spherical model, ζ is given by equation I-25, and ω_{0c} is the value which is utilized in the comparisons to the experimental data.

There are five sets of experimental data to which calculations based on the new model can be compared. These are contained in references 15, 33, 36, 37, and 38. In each of these, the measured resonant frequency, ω_{0m} , and the calculated Q are either given directly or can be obtained from a curve. The data in reference 36, which was collected a decade before any of the other data, have variations which require some interpretation to obtain ω_{0m} and Q. This required interpretation makes the ω_{0m} and Q values obtained from reference 36 less reliable than those obtained from other sources.

Comparisons of the data to the model require that values for a and ϵ be known. In some cases, a and ϵ were measured and the values given. In the other cases, it was possible to determine a indirectly from other data in the report. When values of ϵ were not given, average values were obtained from other sources. Measurements of a and ϵ were all made at atmospheric pressure. There is some question as to what effect increasing depth has on swimbladder volume [e.g. 11, 12]; that is, whether the fish retains a constant swimbladder volume or a constant swimbladder mass (Boyle's Law) or some other, intermediate process. (McCartney and Stubbs [37] assumed an intermediate process, due to the effect of tension in the swimbladder wall.) It is probable that different species react to changing depth in different ways and that different experimental methods can affect the way a fish would normally react. Hence, there are uncertainties in the actual values of a at depth. Since the swimbladder is attached to various other parts of the fish, there is no reason to expect a change in swimbladder volume to cause a uniform change in its linear dimensions. Thus, the uncertainty in a at depth produces a smaller uncertainty in ϵ . Various depth variations in a were examined when comparing the data to the model. However, since the individual researcher is in the best position to interpret his own data, the final comparisons utilized the depth variations chosen by those researchers.

The new model requires values of ξ and s . Since the exact value, or range of values, of ξ is presently unknown and s is quite likely under the control of the individual fish, direct comparisons of the model and

experimental data are not possible. However, indirect comparisons are possible. The first step in a comparison is to determine the experimental values of ω_{0m} , Q , a , and ε . Then ω_{0c} is set equal to ω_{0m} and s is calculated utilizing equations IV-1 and IV-18 and figure 1. If surface tension has a negligible effect on ω_{0m} , s can be assumed to be equal to 10^4 dyne/cm, based on the data given in Appendix A. Q_{rad} and Q_{th} are then calculated from equations IV-4 and IV-6 and Q_{vis} is determined from the equation:

$$\frac{1}{Q} = \frac{1}{Q_{rad}} + \frac{1}{Q_{vis}} + \frac{1}{Q_{th}} \quad (IV-19)$$

Finally, ξ is calculated from equation IV-5. The results of this procedure are given in Table II, where L is the fish length, D , a , ω_{0m} , and Q are experimental data, and s and ξ are calculated by equating the model to the data.

The new model can be indirectly compared to the experimental data by examining the values of s and ξ given in Table II. The values shown in Table II are within the limits chosen in Appendix A to give reasonable ranges for s and ξ . This is a necessary condition for the model to be valid, but it is by no means a sufficient condition. In order that the model can be used with some degree of confidence to predict resonant scattering from swimbladder-bearing fish, the variations in s and ξ shown in Table II must also be explained.

The five sets of data can be separated into two groups, based upon the magnitude of tension in the swimbladder wall. Swimbladder tension had little or no effect on the measurements made by Coate, Batzler and Pickwell, and Sundnes and Sand, where $s < 10^5$ dyne/cm. Swimbladder tension appears to have had a significant effect on the measurements by McCartney and Stubbs and Sand and Hawkins, where

$$2 \times 10^5 \text{ dyne/cm} \leq s \leq 4 \times 10^6 \text{ dyne/cm.}$$

Table II — Experimental Data and Results of Comparisons to the New Model

Source	Fish	L cm	D m	a cm	ω_{0m} rad/sec	Q	s dyne/cm	ξ poise
Coate [36]	Crappie	20	4.6	1.10	2400	4.6	10^4	300
Batzler and Pickwell [15]	Goldfish	7	6	0.51	5650	5.1	6×10^4	130
	Goldfish	6	6	0.44	6600	3.8	5×10^4	160
	Anchovy	11	6	0.40	8000	4.5	7×10^4	130
McCartney and Stubbs [37]	Coalfish	30	10	1.17	4150	1.1	1.7×10^6	2600
			20	1.08	5200	1.7	1.9×10^6	1750
			30	1.03	6000	2.5	1.7×10^6	1200
	Pollack	35	30	1.13	4800	1.4	3.6×10^5	2200
			40	1.09	5800	1.3	6.1×10^5	2600
	Ling	55	30	1.60	3150	2.5	8×10^5	1500
	Cod	35	30	1.52	3500	2.0	1.6×10^6	2000
Sand and Hawkins [33]	Cod	16	11	0.69	10700	1.0	3.8×10^6	2500
			25	0.58	8000	1.3	2.8×10^5	1000
			30	0.55	8800	1.6	2.1×10^5	830
			35	0.53	9900	2.2	3.3×10^5	610
			40	0.51	10900	2.5	3.8×10^5	540
			45	0.50	12000	3.2	5.1×10^5	430
			50	0.48	12800	3.5	4.7×10^5	370
Sundnes and Sand [38]	Charr	40	2	0.95	3000	5.2	10^4	240
	(Averages for 5 fish)		6	0.87	4000	4.5	10^4	300
			10	0.80	4900	5.0	10^4	280
			15	0.74	5800	6.1	10^4	220

Goldfish, anchovies, and charr are physostomes, that is, their swimbladders have an opening into their stomachs. Hence, based on consideration of equation II-115, it is to be expected that the tension in physostome swimbladders would be relatively low. The data show that this is so. The other fish are physoclists, that is, their swimbladders are completely closed. These fish may well obtain some benefit, either hydrostatic or otherwise, by maintaining a tension in the swimbladder wall. The data indicate that cod, ling, pollack, and coalfish maintained relatively high values of s . Physiologically, it should be possible for a physoclist to vary the tension in the swimbladder wall from very taut to flaccid. It appears that the crappie swimbladder was in a flaccid condition.

Since physoclists probably can vary the tension in their swimbladders, any shock to their systems, such as a rapid increase in pressure, might cause the swimbladder tension to change dramatically. This seems to be the situation for the cod examined by Sand and Hawkins. This fish had been allowed to become adapted to a depth of 11 m for at least 48 hours. At this depth, its measured resonant frequency was several times higher than that of a bubble of the same presumed size and shape. This difference was attributed to a high swimbladder tension. Rapidly shifting this fish to a depth of 25 m significantly decreased the measured resonant frequency to a value only about 10 percent greater than that expected for a bubble of the same presumed size and shape. This ratio remained essentially constant as the fish was shifted in 5 m increments to 50 m. The decrease in ω_{0m} as the fish was shifted from 11 m to 25 m is readily explained by the new model by a sudden decrease in s , which seems quite feasible from a physiological standpoint.

Thus, the variations in the values of s calculated using the new model can be explained by the differences between physostomes and physoclists and by the ability of physoclists to vary swimbladder tension. Hence, the new model is an improvement over the models of Andreeva and Lebedeva. By using a variable swimbladder tension, rather than a fixed shear modulus, to model tissue stiffness, the new model can predict resonant frequencies significantly higher than those expected for a free bubble, whereas the other models cannot.

As a practical matter, a parameter that can be randomly varied over several orders of magnitude is not very useful in a predictive model. However, the variations in tension indicated in Table II were obtained from fish which were subjected to other than natural conditions, such as rapid changes in depth. It is quite possible that, under more natural conditions, values of swimbladder tension would be much more uniform. Thus, it could very well be that further experiments, in which the experimental conditions more closely approximate natural conditions, could provide much information about swimbladder tension. This would enhance the value of the new model as a predictor of resonance in large physoclists.

Although the variations in s can be adequately explained by variations in fish physiology, the uncertain variation of s with depth definitely causes some degree of variation in s . In order to calculate s , the difference between ω_{0m} and ω_0 for a bubble of the same assumed size and shape is required. Thus, the accuracy of the estimate of ω_{0m} greatly affects the accuracy of the calculated value of s .

Sundnes and Sand measured the resonant frequencies of charr in order to determine their swimbladder volumes. In the case of these physostomes, this was a valid procedure. However, in the case of large physoclists, where swimbladder tension affects ω_{0m} , this procedure would be invalid. Hence, experiments which might be designated to acoustically examine swimbladder tension require an accurate and independent measurement of swimbladder volume at depth.

The values of ξ given in Table II are also grouped on the basis of the magnitude of swimbladder tension. For the cases where

$$s < 10^5 \text{ dyne/cm},$$

the values of ξ range from 130 to 300 poise, with the values being quite consistent for a particular set of data. For the cases where

$$s > 2 \times 10^5 \text{ dyne/cm},$$

the values of ξ range from 370 to 2,600 poise, with wide variations within a particular set of data. Based on the consistent results obtained, and the reasonableness of their values, it appears that the new model can be used to predict the damping for the first group. However, the high values and variability of ξ in the second group must be examined more closely before any conclusion can be reached.

There are essentially two sources of the variations in the calculated values of ξ between the two groups and within the group where $s > 2 \times 10^5$ dyne/cm. One source is the experimental data and the other is the model. The most likely, and probably greatest, source of error in the experimental data is the uncertainty in swimbladder volume. Since the calculated values of ξ are proportional to a^2 , an error in a can cause a large error in ξ . However, as mentioned earlier, the experimental data were examined assuming various swimbladder volume-depth relationships. None of these relationships produced consistent results or values as low as those obtained for the first group, although in some cases the variability was reduced. For example, if a constant $a = 0.69$ cm is assumed for the cod examined by Sand and Hawkins, ξ varies from 1,500 to 900 poise as the depth increases from 25 to 50 m. This variation is smaller than that for the swimbladder-depth relationship which was utilized, but the values are still much higher than those of the first group and are by no means consistent. It is possible, though, that the cod-like fish, which have a well-developed muscle system, have an intrinsically higher tissue viscosity than fish such as goldfish or anchovies.

At the beginning of this chapter, it was assumed that

$$\xi \leq 2 \times 10^3 \text{ poise}$$

and the equations were simplified accordingly. It might be suspected that this could be a source of error in the cases where $\xi > 2 \times 10^3$ poise. However, the error caused by simplifying equations III-26 and III-34 to equations IV-1 and IV-2 is less than ten percent for values as high as $\xi = 6 \times 10^3$ poise. Thus, the simplified equations are not a significant source of error.

The other primary source of error is the model itself. Since it does not seem to be possible to attribute all the variations in ξ to the errors in the data, it appears that the remaining variations are due to inadequacies in the model.

An examination of all the data in Table II indicates that ξ generally increases with s . There is no indication that this is so for the group of data for which $s < 10^5$ dyne/cm. However, there is definite correlation between s and ξ when the two groups of data are compared. Also, despite the wide variations of ξ within the group of data for which $s > 2 \times 10^5$ dyne/cm, there is a rough indication that ξ increases with s for this group of data. Thus, it appears that increasing tension in the swimbladder wall has little or no effect on ξ for $s < 10^5$ dyne/cm, but that it does cause ξ to increase for $s > 2 \times 10^5$ dyne/cm. The apparent increase in viscosity with increasing tension in the swimbladder wall for $s > 2 \times 10^5$ dyne/cm would not be expected to occur in a Newtonian fluid. This indicates that modelling a fish as a Newtonian fluid may not be appropriate for $s > 2 \times 10^5$ dyne/cm and that some type of non-Newtonian model, such as a dilatant or viscoelastic fluid, may be more appropriate. However, the present model is appropriate for $s < 10^5$ dyne/cm.

CHAPTER V

CONCLUSIONS

The new model of a swimbladder-bearing fish as a viscous shell enclosing an air cavity with surface tension at the inner interface was developed because older models, of which Andreeva's model [26] is most widely employed, do not accurately predict the results obtained in experiments on the characteristics of swimbladder resonance. The principal difference between the older models and the data is that the values of Q predicted by the models are always higher than those obtained experimentally. A second difference is that the older models can not account for the high resonant frequencies obtained for some large physoclists. The new model sought to correct these differences by explicitly including the viscosity of fish tissue and by including a tension in the swimbladder wall.

For convenience, the equations developed for the new model will be restated here:

$$\omega_0^2 a^2 = \frac{3\gamma_a P_{0w}}{\rho_{0f}} + \frac{2s}{\rho_{0f} a} (3\gamma_a - 1) \quad (V-1)$$

$$\sigma = \frac{4\pi a^2 \left(\frac{\rho_{0w}}{\rho_{0f}} \right)^2}{\left[\frac{\omega_0^2}{\omega^2 H^2} + \left(\frac{\omega_0^2}{\omega^2} - 1 \right)^2 \right]} \quad (V-2)$$

$$H_{rad} = \frac{\omega_0 \rho_{0f} c_w}{\omega^2 \rho_{0w} a} \quad (V-3)$$

$$H_{vis} = \frac{\omega_0 \rho_{0f} a^2}{2\xi} \quad (V-4)$$

and

$$H_{th} = \frac{\omega_0 a}{3(\gamma_a - 1)} \left(\frac{2\rho_{0a} c_{pa}}{\omega \kappa_a} \right)^{1/2} \left(1 + \frac{2s}{\rho_{0f} \omega^2 a^3} \right)^{-1} \quad (V-5)$$

Comparable equations for an air bubble in water are available at only $\omega = \omega_0$, where $H = Q$. The equations for σ and Q obtained for the new model are essentially the same as those for an air bubble in water, the only significant difference being in the value of the viscosities of fish flesh and water. However, the equations for ω_0 for the new model and an air bubble in water for which viscosity and surface tension are included are not the same. If the viscosity of fish flesh were used in the equation obtained for an air bubble, ω_0 could be zero or imaginary. However, for the new model, the effect of viscosity on ω_0 was shown to be small enough to be neglected.

Equations V-1 and V-2 are valid for an upper limit for $\xi = 6 \times 10^3$ poise. If $\xi > 6 \times 10^3$ poise, then the outer shell radius, b , appears in the σ -equation. This implies that this is a boundary layer-type problem. Thus, if the fish flesh-water interface is outside the boundary layer, the magnitude of b is immaterial.

All of the models are spherical in nature. However, the swimbladders of some fish are sufficiently elongated that their shapes can have a significant effect on ω_0 . Thus, equation V-1 should be modified to include this effect. Hence:

$$\omega_0^2 a^2 = \zeta \left[\frac{3\gamma_a P_{0w}}{\rho_{0f}} + \frac{2s}{\rho_{0f} a} (3\gamma_a - 1) \right] \quad (V-6)$$

Although ζ was determined for a bubble in water, its use here is quite reasonable, especially when the similarity between the equations for a bubble and the new model are considered.

Several other conclusions can be reached for the new model. One is that, for the ratios of outside to inside shell diameters considered, the actual value of the outside diameter has no effect on the results. Another is that thermal losses are not very significant and, in most cases, can be neglected. A third is that, for low values of H , $(\omega_0/\omega H)^2$ can be comparable to $[(\omega_0^2/\omega^2) - 1]^2$ at off-resonant frequencies. Hence, considering the experimental values of Q obtained, it is apparent that H , rather than Q , should be used to calculate σ .

A comparison of the new model with available experimental data indicates that the new model constitutes a definite improvement over previous models. The new model can predict low values of Q and elevated values of ω_0 which the previous models could not. In addition, the new model can be used to obtain the magnitude of damping at any frequency, whereas many previous models only produced the value at resonance.

The comparison of the new model with experimental data indicates that the model is most accurate for fish in which $s < 10^5$ dyne/cm. Table II indicates that this includes physostomes up to at least 40 cm in length. In addition, Appendix A indicates that small physoclists, 10 cm or less in length, are also included in this group. Most of the fish found in deep scattering layers are smaller than 10 cm and none have the well developed musculature of fish such as cod. Thus, it appears that the new model will be of considerable value in studies of volume reverberation. Table II indicates that a value of ξ of approximately 200 poise is appropriate for these studies.

The variations in s and ξ required to match the values calculated using the new model to the experimental data for large physoclists indicate that the new model is not completely adequate for these fish. Even so, the new model is still better than previous models and, as such, is of some value in studies of resonance of large physoclists. Table II indicates that values of $s = 10^6$ dyne/cm and 10^3 poise $\leq \xi \leq 2 \times 10^3$ poise should give reasonable results for these studies.

The new model introduces two new parameters, ξ and s . Few measurements of these parameters exist and those that do vary widely. The accuracy of the new model could be determined with much more confidence if better information on ξ and s were available. In addition, the variations of swimbladder volume with depth for different fish species are required for all models. Hence, further experiments to determine s , ξ , and swimbladder size and shape versus depth are recommended. This recommendation is made with the realization that the complexities involved in these experiments will be significant.

REFERENCES

1. C.F. Eyring, R.J. Christensen, and R.W. Raitt, "Reverberation in the Sea," J. Acoust. Soc. Am. 20, 462-475 (1948).
2. R.W. Raitt, "Sound Scatterers in the Sea," J. Marine Res. 7, 393-409 (1948).
3. R.S. Dietz, "Deep Scattering Layer in the Pacific and Antarctic Oceans," J. Marine Res. 7, 430-442 (1948).
4. J.B. Hersey and H.B. Moore, "Progress Report on Scattering Layer Observations in the Atlantic Ocean," Am. Geophys. Union Trans. 29, 341-354 (1948).
5. M.W. Johnson, "Sound as a Tool in Marine Ecology, from Data on Biological Noises and the Deep Scattering Layer," J. Marine Res. 7, 443-458 (1948).
6. V.M. Albers, *Underwater Acoustics Handbook-II* (Pennsylvania State University, University Park, PA, 1965) p. 47.
7. N.B. Marshall, "Bathypelagic Fishes as Sound Scatterers in the Ocean," J. Marine Res. 10, 1-17 (1951).
8. J.B. Hersey, H.R. Johnson, and L.C. Davis, "Recent Findings about the Deep Scattering Layer," J. Marine Res. 11, 1-9 (1952).
9. J.B. Hersey and R.H. Backus, "New Evidence that Migrating Gas Bubbles, Probably the Swimbladders of Fish, are Largely Responsible for Scattering Layers on the Continental Rise South of New England," Deep-Sea Res. 1, 190-191 (L) (1954).
10. H.R. Johnson, R.H. Backus, J.B. Hersey, and D.M. Owen, "Suspended Echo-Sounder and Camera Studies of Midwater Sound Scatterers," Deep-Sea Res. 3, 266-272 (1956).
11. J.B. Hersey, R.H. Backus and J. Hellwig, "Sound-Scattering Spectra of Deep Scattering Layers in the Western North Atlantic Ocean," Deep-Sea Res. 8, 196-210 (1962).
12. G.B. Farquhar, Ed., *Proceedings of an International Symposium on Biological Sound Scattering in the Ocean*, Rep. 005 (Maury Center for Ocean Sci., Washington, DC, 1970).
13. S. Machlup and J.B. Hersey, "Analysis of Sound-Scattering Observations from Non-Uniform Distributions of Scatterers in the Ocean," Deep-Sea Res. 3, 1-22 (1955).
14. R.J. Urick, *Principles of Underwater Sound for Engineers* (McGraw-Hill, New York, 1967), p. 188.
15. W.E. Batzler and G.V. Pickwell, "Resonant Acoustic Scattering from Gas-Bladder Fishes," in *Proceedings of an International Symposium on Biological Sound Scattering in the Ocean*, Rep. 005, G.B. Farquhar, Ed. (Maury Center for Ocean Sci., Washington, DC, 1970), pp 168-179.
16. F.R.H. Jones and G. Pearce, "Acoustic Reflection Experiments with Perch (*Perca fluviatilis* Linn.) to Determine the Proportion of the Echo Returned by the Swimbladder," J. Exp. Biol. 35, 437-450 (1958).
17. M. Minnaert, "On Musical Air-Bubbles and the Sounds of Running Water," Phil. Mag. 16, 235-248 (1933).
18. "Physics of Sound in the Sea, Part IV," Nat. Defense Res. Comm. Div. 6 Sum. Tech. Rep. 8, Chap 28, pp 460-467 (1946).
19. C. Devin, Jr., "Survey of Thermal, Radiation, and Viscous Damping of Pulsating Air Bubbles in Water," J. Acoust. Soc. Am. 31, 1654-1667 (1959).
20. A.I. Eller, "Damping Constants of Pulsating Bubbles," J. Acoust. Soc. Am 47, 1469-1470(L) (1970).
21. W.M. Fairbank, Jr., "Damping Constants for Nonresonant Bubbles," J. Acoust. Soc. Am. 58, 746(L) (1975).
22. H.B. Briggs, J.B. Johnson, and W.P. Mason, "Properties of Liquids at High Sound Pressure," J. Acoust. Soc. Am. 19, 664-677 (1947).
23. G. Houghton, "Theory of Bubble Pulsation and Cavitation," J. Acoust. Soc. Am. 35, 1387-1393 (1963).
24. A. Shima, "The Natural Frequency of a Bubble Oscillating in a Viscous Compressible Liquid," ASME J. Basic Eng. 92, 555-562 (1970).
25. D.Y. Hsieh, "Variational Method and Nonlinear Oscillation of Bubbles," J. Acoust. Soc. Am. 58, 977-982 (1975).
26. I.B. Andreeva, "Scattering of Sound by Air Bladders of Fish in Deep Sound-Scattering Ocean Layers," Sov. Phys. Acoust. 10, 17-20 (1964).

27. L.P. Lebedeva, "Measurements of the Dynamic Complex Shear Modulus of Animal Tissues," *Sov. Phys. Acoust.* 11, 163-165 (1965).
28. E. Meyer, K. Brendel, and K. Tamm, "Pulsation Oscillations of Cavities in Rubber," *J. Acoust. Soc. Am.* 30, 1116-1124 (1958).
29. L.P. Lebedeva, "Sound Scattering by Fish," *J. Ichthyology* 12, 144-149 (1972).
30. M. Strasberg, "Gas Bubbles as Sources of Sound in Liquids," *J. Acoust. Soc. Am.* 28, 20-26 (1956).
31. R.L. Capen, "Swimbladder Morphology of Some Mesopelagic Fishes in Relation to Sound Scattering," Naval Electronics Lab. Report 1447, San Diego (March 1967).
32. R.H. Gibbs, Jr., R.H. Goodyear, R.C. Kleckner, C.F.E. Roper, M.J. Sweeney, B.J. Zahuranec, and W.L. Pugh, "Mediterranean Biological Studies, Final Report," Smithsonian Inst. Washington, DC (July 1972).
33. O. Sand and A.D. Hawkins, "Acoustic Properties of the Cod Swimbladder," *J. Exp. Biol.* 58, 797-820 (1973).
34. M. Strasberg, "The Pulsation Frequency of Nonspherical Gas Bubbles in Liquids," *J. Acoust. Soc. Am.* 25, 536-537 (1953).
35. D.E. Weston, "Sound Propagation in the Presence of Bladder Fish," in *Underwater Acoustics*, V.M. Albers, Ed. (Plenum, New York, 1967), Vol. 2, Chap. 5, pp. 55-88.
36. M.M. Coate, "Effect of a Single Fish on Low Frequency Sound Propagation," Naval Ordnance Lab. Report 4514, White Oak, MD (April 1957).
37. B.S. McCartney and A.R. Stubbs, "Measurements of the Target Strength of Fish in Dorsal Aspect, Including Swimbladder Resonance," in *Proceedings of an International Symposium on Biological Sound Scattering in the Ocean*, Rep. 005, G.B. Farquhar, Ed. (Maury Center for Ocean Sci., Washington, DC, 1970), pp. 180-211.
38. G. Sundnes and O. Sand, "Studies of a Physostome Swimbladder by Resonance Frequency Analyses," *J. Cons. Int. Explor. Mer.* 36, 176-182 (1975).
39. W.N. Tavolga, "Sonic Characteristics and Mechanisms in Marine Fishes," in *Marine Bio-Acoustics*, W.N. Tavolga, Ed. (Pergamon Press, New York, 1964) pp. 195-211.
40. A.N. Popper, "The Response of the Swimbladder of the Goldfish (*Carassius auratus*) to Acoustic Stimuli," *J. Exp. Biol.* 60, 295-304 (1974).
41. R.H. Love, "Predictions of Volume Scattering Strengths from Biological Trawl Data," *J. Acoust. Soc. Am.* 57, 300-306 (1975).
42. L.E. Kinsler and A.R. Frey, *Fundamentals of Acoustics* (Wiley, New York, 1962), 2nd Ed.
43. M. Jakob and G.A. Hawkins, *Elements of Heat Transfer* (Wiley, New York, 1957), 3rd Ed., p. 10.
44. H.U. Sverdrup, M.W. Johnson, and R.H. Fleming, *The Oceans: Their Physics, Chemistry, and General Biology* (Prentice-Hall, Englewood Cliffs, N.J., 1942), Chap. 3, pp. 47-97.
45. F.V. Hunt, "Propagation of Sound in Fluids," in *American Institute of Physics Handbook*, D.E. Gray, Ed. (McGraw-Hill, New York, 1963), 2nd Ed., Sect. 3c, pp. 3-28 to 3-59.
46. P.S. Epstein and R.R. Carhart, "The Absorption of Sound in Suspensions and Emulsions. I. Water Fog in Air," *J. Acoust. Soc. Am.* 25, 553-565 (1953).
47. P.M. Morse and H. Feshbach, *Methods of Theoretical Physics*, (McGraw-Hill, New York, 1953), Part 1, Chap. 1, pp. 1-118.
48. O.D. Kellogg, *Foundations of Potential Theory*, (Dover, New York, 1953), p. 156.
49. P.M. Morse and K.U. Ingard, *Theoretical Acoustics*, (McGraw-Hill, New York, 1968), Chap. 8, pp. 400-466.
50. F.W. Sears and M.W. Zemansky, *University Physics*, (Addison-Wesley, Reading, MA., 1955), 2nd Ed., Chap. 13, pp. 224-236.
51. W.T. Thomson, *Vibration Theory and Applications* (Prentice-Hall, Englewood Cliffs, N.J., 1965), Chap. 2, pp. 36-50.

APPENDIX A

PHYSICAL PROPERTIES OF FISH

Several of the physical properties of fish flesh which must be known for this study have not been accurately measured. In this appendix, the available data will be discussed and, where necessary, appropriate approximations determined. Properties which must be specified include compressional wave velocity (or sound velocity), c_t ; density, ρ_{of} ; specific heat at constant pressure, c_{pf} ; ratio of specific heats, γ_f ; thermal conductivity, κ_f ; shear viscosity, η_{sf} ; and bulk viscosity, η_{bf} . In addition, the ratio of swimbladder volume to total fish volume and the surface tension, s , at the air-fish flesh interface must be determined.

Experimental evidence indicates that swimbladder volumes of small mid-water fishes range from about 0.5 to 5 percent of the total fish volume [32]. For larger, near surface marine fishes, swimbladder volumes are about 4 to 5 percent of the total fish volume [A1]. For small fish, the ratio of outer radius, b , to inner radius, a , of the fish flesh shell is chosen to be $2.5 \leq b/a \leq 6$, which corresponds to swimbladder percentage volumes of about 6 to 0.5 percent. For large fish, b/a is chosen to be $2.5 \leq b/a \leq 3.2$, which corresponds to swimbladder percentage volumes of about 6 to 3 percent. The fish size range of interest is about 1 cm to 1 m, which roughly corresponds to $0.1 \text{ cm} \leq a \leq 5 \text{ cm}$ [32, A2, A3].

The acoustic properties of fish flesh have been measured by several researchers [31, A1, A4-A6]. Experimental values of density range from about 1.02 to 1.09 gm/cm³, with an average of about 1.05 gm/cm³. Experimental sound velocities range from about 1.50×10^5 to 1.60×10^5 cm/sec, with an average of 1.55×10^5 cm/sec. The average values are used in this report.

Measurements on the thermal properties of fish flesh are not available. However, data on the thermal conductivity and specific heat at constant pressure of human and dog tissue do exist [A-7]. These data provide sufficiently close approximations to the required values. Thus, for fish tissue

$$c_{pf} = 0.89 \frac{\text{cal}}{\text{gm}^\circ\text{C}}$$

and

$$\kappa_f = 1.32 \times 10^{-3} \frac{\text{cal}}{\text{cm sec } ^\circ\text{C}}.$$

These values are quite close to those for sea water of 35 parts per thousand salinity, which are [45]

$$c_{pw} = 0.93 \frac{\text{cal}}{\text{gm}^\circ\text{C}}$$

and

$$\kappa_w = 1.34 \times 10^{-3} \frac{\text{cal}}{\text{cm sec } ^\circ\text{C}}.$$

Also for sea water [45],

$$\gamma_w \approx 1.01.$$

Thus, it will be assumed that, since other thermal properties of flesh and sea water are very similar,

$$\gamma_f \approx 1.01.$$

Both the shear viscosity, η_{sf} , and the bulk viscosity, η_{bf} , are required for the present model. However, for convenience, a viscosity parameter, ξ , will be defined as

$$\xi = 4/3 \eta_{sf} + \eta_{bf}. \quad (\text{A-1})$$

The ratio, η_{bf}/η_{sf} , for animal tissue is similar to that for water, which is approximately 3 [A8, A9]. Thus,

$$\xi \approx 4.3 \eta_{sf} \approx 1.4 \eta_{bf}. \quad (\text{A-2})$$

Only one set of data on the viscosity of animal tissue is available. However, other data exist from which tissue viscosity can be determined indirectly. These data are measurements of absorption, complex shear modulus, and cell viscosity of animal tissue. In all cases it will be assumed that the viscosity of all animal flesh is approximately equal.

The direct measurements of viscosity were performed on mammalian tissue [A10]. η_{sf} was determined by four different methods. The results ranged from 100 to 420 poise, with an average value of 175 poise. Thus the values for ξ range from 430 to 1800 poise, with an average value of 760 poise.

Viscosity can be determined from measurements of absorption of sound by utilizing the equation [A11]:

$$\xi = \frac{2\rho_0 c^3 \alpha}{\omega^2} \quad (A-3)$$

where α is the absorption and ω the circular frequency. Many measurements of absorption in tissue have been made at high frequencies. However, tissue exhibits relaxation phenomena at high frequencies so that viscosities at frequencies above relaxation cannot be directly related to those below and can be used only as lower limits. It has been found that for muscle, η_s relaxes near 400 kHz and η_b relaxes near 40 kHz [A12]. Only one set of absorption measurements has been conducted below the Megahertz range. These measurements were made at 300 to 350 kHz [A13]. Utilizing equation A-3, ξ was calculated from these data to range from 30 to 220 poise, with an average value of 130 poise. However, η_b has already relaxed at the measurement frequencies, so that its contribution to the absorption is unknown. Thus, equation A-3 provides a lower limit to ξ . An upper limit can be determined for ξ if it is assumed that the absorption is due solely to η_s . Then, at lower frequencies, ξ would range from 130 to 950 poise, with an average value of 580 poise. Thus, from the absorption measurements:

$$30 \text{ poise} \leq \xi \leq 950 \text{ poise.}$$

Viscosity can also be estimated from measurements of complex shear modulus by utilizing the equation [A9]:

$$\eta_s = \frac{\mu_i}{\omega} \quad (A-4)$$

where μ_i is the imaginary part of the complex shear modulus. One set of measurements of the complex shear modulus of fish tissue has been made from about 2 to 14 kHz [27]. Utilizing equations A-4 and A-1, ξ was calculated from these data to range from about 4 to 90 poise, with an average value of 28 poise.

The viscosity of animal tissue can also be estimated from the viscosity of animal cells if it is assumed that the tissue viscosity is equivalent to the cell viscosity. Separate measurements have been made on the viscosities of both cell protoplasm and membrane. Thus, to estimate the viscosity of the complete cell, a geometric average of the membrane and protoplasmic viscosities is calculated based on the proportional thicknesses of membrane and protoplasm. The equation used to calculate cell viscosity is

$$\xi_c = \left[\frac{a(b-a)}{b^2} \xi_p \xi_m \right]^{1/2} \quad (A-5)$$

where ξ_c , ξ_p and ξ_m are the viscosity parameters of the cell, protoplasm and membrane, respectively, and a and b are the inner and outer membrane radii. Cell radii range from 2×10^{-4} to 15×10^{-4} cm and cell membranes are 75×10^{-8} to 10^{-6} cm thick [A14]. Thus

$$5 \times 10^{-4} \leq \frac{b-a}{b} \leq 5 \times 10^{-3},$$

and $a/b \approx 1$. Measurements have been made on η_s of protoplasm and η_b of membranes. For protoplasm, η_s was found to range from 4×10^{-2} to 3×10^{-1} poise [A15]. For membranes, η_b was found to range from 2.7×10^7 to 2.7×10^8 poise [A16]. Therefore, utilizing equations A-2 and A-5,

$$60 \text{ poise} \leq \xi_c \leq 1,600 \text{ poise.}$$

This estimate is probably subject to the greatest error of the three indirect estimates of viscosity due to all the assumptions required.

Summarizing the ranges of ξ determined by the various methods in their probable order of accuracy: direct measurement,

$$430 \text{ poise} \leq \xi \leq 1,800 \text{ poise;}$$

absorption,

$$30 \text{ poise} \leq \xi \leq 950 \text{ poise;}$$

complex shear modulus,

$$4 \text{ poise} \leq \xi \leq 90 \text{ poise;}$$

cell viscosity,

$$60 \text{ poise} \leq \xi \leq 1,600 \text{ poise.}$$

The total range of data is

$$4 \text{ poise} \leq \xi \leq 1,800 \text{ poise.}$$

Thus, for this study, limits of

$$1 \text{ poise} \leq \xi \leq 10^4 \text{ poise}$$

will be used, with a more likely range being

$$50 \text{ poise} \leq \xi \leq 2 \times 10^3 \text{ poise.}$$

The swimbladder wall of a fish is a membrane which is capable of supporting tension. In the present model, the swimbladder wall has zero thickness, so that the tension in the membrane is effectively a surface tension. Measurements of the internal swimbladder pressure can be used to calculate surface tension since

$$\Delta P = (2s/a), \quad (\text{A-6})$$

where ΔP is the difference between the internal swimbladder pressure and the ambient pressure [50]. Several researchers have measured internal swimbladder pressures, but since it is probable that a fish can control the tension in the swimbladder wall, only measurements on live, unanesthetized, fish are considered. Excess internal pressures from 2×10^4 to 6×10^5 dynes/cm² have been measured in fishes which were 2 to 20 cm long [A17]. These results correspond to surface tensions of 6×10^3 to 7×10^4 dyne/cm for fish with swimbladder radii of about 0.1 to 1.0 cm. The majority of these fish were less than 10 cm long with swimbladder radii less than 0.5 cm.

Surface tension is probably a function of fish size, so that measurements on larger fish are needed for the present study. No measurements of excess pressure of larger, unanesthetized fish are available. However, another means can be used to estimate the upper limits of surface tension in larger fishes. As discussed in the text, Sand and Hawkins have attributed high experimental resonant frequencies to swimbladder tension [33]. If this is true, then an upper limit of surface tension can be calculated by assuming that the fish is a free bubble with surface tension and utilizing equation I-12, neglecting viscosity, and equation I-25 to account for spheroidal swimbladder shapes. Although this method does not necessarily give accurate estimates of surface tension, it does produce values which can be used as upper limits. These limits are useful because it is the possible range of surface tension that is required. Surface tensions calculated from resonance measurements range from about 10^6 to 10^8 dyne/cm for swimbladder radii from 1 to 2.5 cm [33,37].

The surface tension of an air bubble in water is 74 dyne/cm [50]. Hence, the range of surface tension for small swimbladders ($a \approx 0.1$ cm) is chosen to be

$$10^2 \text{ dyne/cm} \leq s \leq 10^6 \text{ dyne/cm.}$$

For larger swimbladders ($a \approx 5$ cm) the range is chosen to be

$$10^2 \text{ dyne/cm} \leq s \leq 10^8 \text{ dyne/cm.}$$

APPENDIX A REFERENCES

- A1. F.R.H. Jones and N.B. Marshall, "The Structure and Functions of the Teleostean Swimbladder," *Biol. Rev.* 28, 16-83 (1963).
- A2. R.W.G. Haslett, "Measurement of the Dimensions of Fish to Facilitate Calculations of Echo-Strength in Acoustic Fish Detection," *J. Cons. Int. Explor. Mer* 27, 261-269 (1962).
- A3. R.H. Love, "Maximum Side-Aspect Target Strength of an Individual Fish," *J. Acoust. Soc. Am.* 46, 746-752 (1969).
- A4. E.V. Shishkova, "Investigation of the Acoustic Properties of the Bodies of Fish," *Tr. Vses. Nauchn.-issled. Inst. Morsk. Rybn. Khoz. Okeanogr.* 36, 259-269 (1958). [English Transl.: Associated Technical Services, Inc., East Orange, N.J. (1960).]
- A5. M. Freese and D. Makow, "High-Frequency Ultrasonic Properties of Freshwater Fish Tissue," *J. Acoust. Soc. Am.* 44, 1282-1289 (1968).
- A6. R.W.G. Haslett, "The Back-Scattering of Acoustic Waves in Water by an Obstacle II: Determination of the Reflectivities of Solids Using Small Specimens," *Proc. Phys. Soc.* 79, 559-571 (1962).
- A7. T.E. Cooper and G.J. Trezek, "A Probe Technique for Determining the Thermal Conductivity of Tissue," *J. Heat Transfer, Trans. ASME* 94, Series C, 133-140 (1972).
- A8. W.D. O'Brien, Jr., Personal communication, April 1974.
- A9. T.A. Litovitz and C.M. Davis, "Structural and Shear Relaxation in Liquids," in *Physical Acoustics*, W.P. Mason, Ed. (Academic Press, New York, 1965) Vol. 2A, Chap. 5, pp. 281-349.
- A10. H.E. von Gierke, H.L. Oestreicher, E.K. Franke, H.O. Parrack and W.W. von Wittern, "Physics of Vibrations in Living Tissues," *J. Appl. Physiol.* 4, 886-900 (1952).
- A11. J. Lamb, "Thermal Relaxation in Liquids," in *Physical Acoustics*, W.P. Mason, Ed. (Academic Press, New York, 1965) Vol. 2A, Chap. 4, pp. 203-280.
- A12. F. Dunn, "Temperature and Amplitude Dependence of Acoustic Absorption in Tissue," *J. Acoust. Soc. Am.* 34, 1545-1547 (1962).
- A13. D.E. Goldman and T.F. Hueter, "Tabular Data of the Velocity and Absorption of High-Frequency Sound in Mammalian Tissues," *J. Acoust. Soc. Am.* 28, 35-37 (1956).
- A14. E.D.P. DeRobertis, W.W. Nowinski, and F.A. Saez, *Cell Biology*, (W.B. Saunders, Philadelphia, 1970), 5th Ed., p. 18, p. 152.
- A15. L.V. Heilbrunn, *An Outline of General Physiology*, (W.B. Saunders, Philadelphia, 1955), 3rd Ed., Chap. 8, pp. 69-88.
- A16. A. Katchalsky, O. Kedem, C. Klibansky, and A. DeVries, "Rheological Considerations of the Haemolysing Red Blood Cell," in *Flow Properties of Blood and Other Biological Systems*, A.L. Copley and G. Stainsby, Eds. (Pergamon Press, New York, 1960).
- A17. J.H. Gee, K. Machniak, and S.M. Chalanchuk, "Adjustment of Buoyancy and Excess Internal Pressure of Swimbladder Gases in Some North American Freshwater Fishes," *J. Fish. Res. Board Can.* 31, 1139-1141 (1974).

APPENDIX B

SIMPLIFIED EXPRESSION FOR (B_w/A)

Simplification of (B_w/A) as given in equation III-16 is based on the ranges of physical properties and the limits of the variables given in Chapter II.

The first step in the simplification of equation III-16 is the simplification of the spherical Bessel, Neumann, and Hankel functions in the S_{ij} 's. In the k_{1a} terms:

$$j_0(k_{1a}a) = \frac{\sin(k_{1a}a)}{k_{1a}a} \quad (B-1)$$

and

$$j_0'(k_{1a}a) = \frac{\cos(k_{1a}a)}{k_{1a}a} - \frac{\sin(k_{1a}a)}{k_{1a}^2 a^2} \quad (B-2)$$

Now, if

$$\sin(k_{1a}a) = \sin[(1+i)xa] , \quad (B-3)$$

then

$$\sin(k_{1a}a) = \sin(xa)\cosh(xa) - i \sinh(xa)\cos(xa) \quad (B-4)$$

Similarly,

$$\cos(k_{1a}a) = \cos(xa)\cosh(xa) - i \sin(xa)\sinh(xa) . \quad (B-5)$$

An examination of the parameters involved shows that $xa > 10$, so that,

$$\cosh(xa) \approx \sinh(xa) \approx \frac{e^{xa}}{2} \quad (B-6)$$

and

$$\sin(k_{1a}a) \approx i \cos(k_{1a}a) . \quad (B-7)$$

Thus,

$$j_0(k_{1a}a) = \frac{i \cos(k_{1a}a)}{k_{1a}a} \quad (B-8)$$

and

$$j_0'(k_{1a}a) = -j_0(k_{1a}a) \left[i + \frac{1}{k_{1a}a} \right] . \quad (B-9)$$

One of the assumptions in the model is that the shell is small compared to the wavelength of the incident compressional wave. This means that $k_{2w}b$, $k_{2t}b$, and $k_{2a}a$ are small. The definition of "small" will now be determined by examining the expansions for spherical functions of small argument:

$$j_0(z) = \left(1 - \frac{z^2}{6} + \dots \right), \quad (B-10)$$

$$j_0'(z) = -\frac{z}{3} \left(1 - \frac{z^2}{10} + \dots \right), \quad (B-11)$$

$$j_0''(z) = -\frac{1}{3} \left(1 - \frac{3z^2}{10} + \dots \right), \quad (B-12)$$

$$n_0(z) = -\frac{1}{z} \left(1 - \frac{z^2}{2} + \dots \right), \quad (B-13)$$

$$n_0'(z) = \frac{1}{z^2} \left(1 + \frac{z^2}{2} - \dots \right), \quad (B-14)$$

$$n_0''(z) = -\frac{2}{z^3} \left(1 + \frac{z^2}{8} - \dots \right), \quad (B-15)$$

$$h_0(z) = \left(1 - \frac{z^2}{6} + \dots\right) - \frac{i}{z} \left(1 - \frac{z^2}{2} + \dots\right), \quad (\text{B-16})$$

$$h_0'(z) = -\frac{z}{3} \left(1 - \frac{z^2}{10} + \dots\right) + \frac{i}{z^2} \left(1 + \frac{z^2}{2} - \dots\right), \quad (\text{B-17})$$

$$h_0''(z) = -\frac{1}{3} \left(1 - \frac{3z^2}{10} + \dots\right) - \frac{2i}{z^3} \left(1 + \frac{z^4}{8} - \dots\right). \quad (\text{B-18})$$

In order to limit errors in these functions to under ten percent, it must be assumed that

$$k_{2w}^2 b^2 < 2 \times 10^{-1}, \quad (\text{B-19})$$

$$k_{2f}^2 b^2 < 2 \times 10^{-1} \quad (\text{B-20})$$

and

$$k_{2a}^2 a^2 < 6 \times 10^{-1}. \quad (\text{B-21})$$

This implies that in fish flesh and water

$$\omega b < 7 \times 10^4 \text{ cm/sec} \quad (\text{B-22})$$

and in air

$$\omega a < 2.4 \times 10^4 \text{ cm/sec}. \quad (\text{B-23})$$

Then with these limitations and the acceptance of at most a ten percent error, equations B-10 through B-18 can be written as:

$$j_0(z) = 1, \quad (\text{B-24})$$

$$j_0'(z) = -\frac{z}{3}, \quad (\text{B-25})$$

$$j_0''(z) = -\frac{1}{3}, \quad (\text{B-26})$$

$$n_0(z) = -\frac{1}{z}, \quad (\text{B-27})$$

$$n_0'(z) = \frac{1}{z^2}, \quad (\text{B-28})$$

$$n_0''(z) = -\frac{2}{z^3}, \quad (\text{B-29})$$

$$h_0(z) = 1 - \frac{i}{z}, \quad (\text{B-30})$$

$$h_0'(z) = -\frac{z}{3} + \frac{i}{z^2}, \quad (\text{B-31})$$

$$h_0''(z) = -\frac{1}{3} - \frac{2i}{z^3}. \quad (\text{B-32})$$

It is necessary to keep both the largest real and largest imaginary term in the spherical Hankel function expansions, regardless of their comparative magnitudes.

Equations B-24 through B-32 will now be utilized to simplify equations III-2 through III-15. In addition, equations II-59, II-60, II-68, and II-69, will be substituted for k_{1a} , k_{2a} , k_{2f} , and k_{2w} . These substitutions yield, after neglecting any term which causes an error of less than ten percent, the following expressions for the S_j 's:

$$S_{11} = \frac{\omega^2 b}{3\rho_{0w} c_w^2} - \frac{i c_w}{\rho_{0w} \omega b^2}. \quad (\text{B-33})$$

$$S_{12} = -\frac{\omega^2 b}{3\rho_{0f} c_f^2} , \quad (B-34)$$

$$S_{13} = \left(\frac{c_f}{\rho_{0f} \omega b^2} \right) \left(1 - \frac{3i\xi\omega}{2\rho_{0f} c_f^2} \right) , \quad (B-35)$$

$$a_1 = -\frac{\omega^2 b}{3\rho_{0w} c_w^2} , \quad (B-36)$$

$$S_{21} = -1 + \frac{ic_w}{\omega b} , \quad (B-37)$$

$$S_{22} = 1 - \frac{i\omega\xi}{3\rho_{0f} c_f^2} , \quad (B-38)$$

$$S_{23} = -\left(\frac{c_f}{\omega b} \right) \left[1 + \frac{3\xi^2}{\rho_{0f}^2 c_f^2 b^2} + \frac{2i\xi}{\rho_{0f} \omega b^2} \right] , \quad (B-39)$$

$$a_2 = 1 , \quad (B-40)$$

$$S_{32} = -\frac{\omega^2 a}{3\rho_{0f} c_f^2} , \quad (B-41)$$

$$S_{33} = \left(\frac{c_f}{\rho_{0f} \omega a^2} \right) \left(1 - \frac{3i\xi\omega}{2\rho_{0f} c_f^2} \right) , \quad (B-42)$$

$$S_{34} = \frac{\omega^2 a}{3\rho_{0a} c_a^2} + (1+i) \left(\frac{\omega}{\rho_{0a} c_a^2} \right) (\gamma_a - 1) \left(\frac{\omega \kappa_a}{2\rho_{0a} c_{pa}} \right)^{1/2} , \quad (B-43)$$

$$S_{42} = 1 - \frac{i\omega\xi}{3\rho_{0f} c_f^2} , \quad (B-44)$$

$$S_{43} = -\left(\frac{c_f}{\omega a} \right) \left[1 + \frac{3\xi^2}{\rho_{0f}^2 c_f^2 a^2} + \frac{2i\xi}{\rho_{0f} \omega a^2} \right] , \quad (B-45)$$

$$S_{44} = -1 + \frac{2s}{3\rho_{0a} c_a^2 a} + \left[\frac{2s(\gamma_a - 1)}{\rho_{0a} c_a^2 \omega a^2} \right] \left(\frac{\omega \kappa_a}{2\rho_{0a} c_{pa}} \right)^{1/2} \\ + i(\gamma_a - 1) \left(\frac{\omega \kappa_a}{\rho_{0a} c_a^2 c_{pa}} \right) \left[1 + \frac{2s}{\omega a^2} \left(\frac{c_{pa}}{2\rho_{0a} \omega \kappa_a} \right)^{1/2} \right] . \quad (B-46)$$

Substitution of equations B-33, B-36, B-37 and B-40 into III-16 yields:

$$\frac{B_w}{A} = \frac{-\left(\frac{\omega^2 b}{3\rho_{0w} c_w^2}\right) U + W}{\left[\frac{\omega^2 b}{3\rho_{0w} c_w^2} - \frac{ic_w}{\rho_{0w} \omega b^2}\right] U - \left[1 - \frac{ic_w}{\omega b}\right] W}, \quad (B-47)$$

or

$$\frac{B_w}{A} = \frac{-Y}{Y - Z}, \quad (B-48)$$

where

$$Y = \left(\frac{\omega^2 b}{3\rho_{0w} c_w^2}\right) U - W, \quad (B-49)$$

and

$$Z = \left(\frac{ic_w}{\omega b}\right) \left[\left(\frac{1}{\rho_{0w} b}\right) U - W\right]. \quad (B-50)$$

The remainder of the simplification process for equation III-16 will be conducted in several steps. In each step, the order of magnitude of the various terms will be compared and terms which cause an error of less than ten percent will be neglected. This procedure will be done in such a way that no term is neglected which could become important due to a later subtraction. It should be mentioned that most of the terms which are neglected result in errors of much less than ten percent and in those cases where the errors approach ten percent, that error is approached only at the limiting values of the terms involved. In order that the simplification process can be checked by the interested reader, the results of each step will be given, rather than just the final result.

The next step is to simplify the terms in the parentheses in equations III-17 and III-18. The results are

$$S_{22}S_{33} - S_{23}S_{32} = \left(\frac{c_l}{\rho_{0l}\omega a^2}\right) - \left(\frac{i\xi}{6\rho_{0l}^2 c_l a^2}\right) \left(11 + \frac{4a^3}{b^3}\right), \quad (B-51)$$

$$S_{23}S_{42} - S_{22}S_{43} = \left(\frac{c_l}{\omega a}\right) \left[\left(1 - \frac{a}{b}\right) + \left(\frac{11\xi^2}{3\rho_{0l}^2 c_l^2 a^2}\right) \left(1 - \frac{a^3}{b^3}\right) + \left(\frac{2i\xi}{\rho_{0l}\omega a^2}\right) \left(1 - \frac{a^3}{b^3}\right)\right], \quad (B-52)$$

$$S_{13}S_{32} - S_{12}S_{33} = \left(\frac{\omega b}{3\rho_{0l}^2 c_l a^2}\right) \left(1 - \frac{a^3}{b^3}\right) - i \left(\frac{\omega^2 \xi b}{2\rho_{0l}^3 c_l^3 a^2}\right) \left(1 - \frac{a^3}{b^3}\right), \quad (B-53)$$

and

$$S_{12}S_{43} - S_{13}S_{42} = \left(\frac{\omega b}{3\rho_{0l} c_l a}\right) + \left(\frac{\omega \xi^2 b}{\rho_{0l}^3 c_l^3 a^3}\right) - \left(\frac{c_l}{\rho_{0l}\omega b^2}\right) + \left(\frac{i\xi}{6\rho_{0l}^2 c_l b^2}\right) \left(11 + \frac{4b^3}{a^3}\right). \quad (B-54)$$

The next apparent step would be to simplify the expressions for U and W. This, however, can lead to errors when the subtractions indicated for Y and Z are made. Hence, the next step is to simplify Y and (Y-Z). Before writing the simplified expressions for Y and (Y-Z), several intermediate steps will be given in order to assist the interested reader in checking the final expressions.

Substitution of equations B-43, B-46, B-51, and B-52 into III-17 yields:

$$\begin{aligned}
 U = & - \left(\frac{c_1}{\rho_{0f} \omega a^2} \right) \left(1 - \frac{2s}{3\rho_{0a} c_a^2 a} \right) + \left[\frac{2s c_1 (\gamma_a - 1)}{\rho_{0f} \rho_{0a} c_a^2 \omega^2 a^4} \right] \left(\frac{\omega \kappa_a}{2\rho_{0a} c_{pa}} \right)^{1/2} \\
 & + \left[\frac{\omega \xi (\gamma_a - 1) \kappa_a}{6\rho_{0f}^2 c_1 \rho_{0a} c_a^2 c_{pa} a^2} \right] \left[1 + \left(\frac{2s}{\omega a^2} \right) \left(\frac{c_{pa}}{2\rho_{0a} \omega \kappa_a} \right)^{1/2} \right] \left(11 + \frac{4a^3}{b^3} \right) \\
 & + \left(\frac{c_1}{\rho_{0a} c_a^2 a} \right) \left\{ \left(\frac{\omega a}{3} \right) \left(1 - \frac{a}{b} \right) + \left(\frac{11\omega \xi^2}{9\rho_{0f}^2 c_1^2 a} \right) \left(1 - \frac{a^3}{b^3} \right) \right. \\
 & + (\gamma_a - 1) \left(\frac{\omega \kappa_a}{2\rho_{0a} c_{pa}} \right)^{1/2} \left(1 - \frac{a}{b} \right) - \left[\frac{2\xi(\gamma_a - 1)}{\rho_{0f} \omega a^2} \right] \left(\frac{\omega \kappa_a}{2\rho_{0a} c_{pa}} \right)^{1/2} \left(1 - \frac{a^3}{b^3} \right) \\
 & + \left. \left[\frac{11\xi^2(\gamma_a - 1)}{3\rho_{0f}^2 c_1^2 a^2} \right] \left(\frac{\omega \kappa_a}{2\rho_{0a} c_{pa}} \right)^{1/2} \left(1 - \frac{a^3}{b^3} \right) \right\} \\
 & + i \left(\frac{\xi}{6\rho_{0f}^2 c_1 a^2} \right) \left(1 - \frac{2s}{3\rho_{0a} c_a^2 a} \right) \left(11 + \frac{4a^3}{b^3} \right) \\
 & - i \left[\frac{\xi s (\gamma_a - 1)}{3\rho_{0a} c_a^2 \rho_{0f}^2 c_1 \omega a^4} \right] \left(\frac{\omega \kappa_a}{2\rho_{0a} c_{pa}} \right)^{1/2} \left(11 + \frac{4a^3}{b^3} \right) \\
 & + i \left[\frac{c_1 (\gamma_a - 1) \kappa_a}{\rho_{0a} c_a^2 \rho_{0f} c_{pa} a^2} \right] \left[1 + \left(\frac{2s}{\omega a^2} \right) \left(\frac{c_{pa}}{2\rho_{0a} \omega \kappa_a} \right)^{1/2} \right] \\
 & + i \left(\frac{c_1}{\rho_{0a} c_a^2 a} \right) \left\{ \left(\frac{2\xi}{3\rho_{0f} a} \right) \left(1 - \frac{a^3}{b^3} \right) + (\gamma_a - 1) \left(\frac{\omega \kappa_a}{2\rho_{0a} c_{pa}} \right)^{1/2} \left(1 - \frac{a}{b} \right) \right. \\
 & + \left. \left[\frac{2\xi(\gamma_a - 1)}{\rho_{0f} \omega a^2} \right] \left(\frac{\omega \kappa_a}{2\rho_{0a} c_{pa}} \right)^{1/2} \left(1 - \frac{a^3}{b^3} \right) \right. \\
 & + \left. \left[\frac{11\xi^2(\gamma_a - 1)}{3\rho_{0f}^2 c_1^2 a^2} \right] \left(\frac{\omega \kappa_a}{2\rho_{0a} c_{pa}} \right)^{1/2} \left(1 - \frac{a^3}{b^3} \right) \right\}. \tag{B-55}
 \end{aligned}$$

Substitution of equations B-43, B-46, B-53, and B-54 into III-18 yields:

$$\begin{aligned}
 W = & \left(\frac{\omega b}{3\rho_{0f}^2 c_1 a^2} \right) \left(1 - \frac{a^3}{b^3} \right) \left\{ - \left(1 - \frac{2s}{3\rho_{0a} c_a^2 a} \right) + \left[\frac{2s(\gamma_a - 1)}{\rho_{0a} c_a^2 \omega a^2} \right] \left(\frac{\omega \kappa_a}{2\rho_{0a} c_{pa}} \right)^{1/2} \right. \\
 & + \left. \left[\frac{3\omega^2 \xi \kappa_a (\gamma_a - 1)}{2\rho_{0a} c_a^2 \rho_{0f} c_1^2 c_{pa}} \right] \left[1 + \left(\frac{2s}{\omega a^2} \right) \left(\frac{c_{pa}}{2\rho_{0a} \omega \kappa_a} \right)^{1/2} \right] \right\} \\
 & + \left(\frac{\omega}{\rho_{0a} c_a^2} \right) \left\{ \left(\frac{\omega^2 b}{9\rho_{0f} c_1} \right) + \left(\frac{\omega^2 \xi^2 b}{3\rho_{0f}^3 c_1^3 a^2} \right) - \left(\frac{c_1 a}{3\rho_{0f} b^2} \right) \right. \\
 & + \left. \left[\frac{\omega b (\gamma_a - 1)}{3\rho_{0f} c_1 a} \right] \left(\frac{\omega \kappa_a}{2\rho_{0a} c_{pa}} \right)^{1/2} \right. \\
 & + \left. \left[\frac{\omega \xi^2 b (\gamma_a - 1)}{\rho_{0f}^3 c_1^3 a^3} \right] \left(\frac{\omega \kappa_a}{2\rho_{0a} c_{pa}} \right)^{1/2} - \left[\frac{c_1 (\gamma_a - 1)}{\rho_{0f} \omega b^2} \right] \left(\frac{\omega \kappa_a}{2\rho_{0a} c_{pa}} \right)^{1/2} \right\}
 \end{aligned}$$

$$\begin{aligned}
& - \left[\frac{\xi(\gamma_a - 1)}{6\rho_{0f}^2 c_f b^2} \right] \left(\frac{\omega \kappa_a}{2\rho_{0a} c_{pa}} \right)^{1/2} \left(11 + \frac{4b^3}{a^3} \right) \Big\} \\
& + i \left(\frac{\omega b}{3\rho_{0f}^2 c_f a^2} \right) \left(1 - \frac{a^3}{b^3} \right) \Big\{ \left(\frac{3\omega\xi}{2\rho_{0f} c_f^2} \right) \left(1 - \frac{2s}{3\rho_{0a} c_a^2 a} \right) \right. \\
& - \left[\frac{3\xi s(\gamma_a - 1)}{\rho_{0a} c_a^2 \rho_{0f} c_f^2 a^2} \right] \left(\frac{\omega \kappa_a}{2\rho_{0a} c_{pa}} \right)^{1/2} \\
& + (\gamma_a - 1) \left(\frac{\omega \kappa_a}{\rho_{0a} c_a^2 c_{pa}} \right) \left[1 + \left(\frac{2s}{\omega a^2} \right) \left(\frac{c_{pa}}{2\rho_{0a} \omega \kappa_a} \right)^{1/2} \right] \Big\} \\
& + i \left(\frac{\omega}{\rho_{0a} c_a^2} \right) \Big\{ \left(\frac{\omega \xi a}{18\rho_{0f}^2 c_f b^2} \right) \left(11 + \frac{4b^3}{a^3} \right) + \left[\frac{\omega b(\gamma_a - 1)}{3\rho_{0f} c_f a} \right] \left(\frac{\omega \kappa_a}{2\rho_{0a} c_{pa}} \right)^{1/2} \\
& + \left[\frac{\xi(\gamma_a - 1)}{6\rho_{0f}^2 c_f b^2} \right] \left(\frac{\omega \kappa_a}{2\rho_{0a} c_{pa}} \right)^{1/2} \left(11 + \frac{4b^3}{a^3} \right) + \left[\frac{\omega \xi^2 b(\gamma_a - 1)}{\rho_{0f}^3 c_f^3 a^3} \right] \left(\frac{\omega \kappa_a}{2\rho_{0a} c_{pa}} \right)^{1/2} \\
& - \left[\frac{c_f(\gamma_a - 1)}{\rho_{0f} \omega b^2} \right] \left(\frac{\omega \kappa_a}{2\rho_{0a} c_{pa}} \right)^{1/2} \Big\} . \tag{B-56}
\end{aligned}$$

Substitution of equations B-55 and B-56 into B-49 yields:

$$\begin{aligned}
(\rho_{0a} c_a^2) Y = & - \left(\frac{\rho_{0a} c_a^2 \omega c_f b}{3\rho_{0w} c_w^2 \rho_{0f} a^2} \right) \left(1 - \frac{2s}{3\rho_{0a} c_a^2 a} \right) + \left(\frac{\omega^3 c_f b}{9\rho_{0w} c_w^2} \right) \left(1 - \frac{a}{b} \right) \\
& + \left(\frac{\rho_{0a} c_a^2 \omega b}{3\rho_{0f}^2 c_f a^2} \right) \left(1 - \frac{2s}{3\rho_{0a} c_a^2 a} \right) \left(1 - \frac{a^3}{b^3} \right) - \left(\frac{\omega^3 b}{9\rho_{0f} c_f} \right) + \left(\frac{\omega c_f a}{3\rho_{0f} b^2} \right) \\
& + \left(\frac{11\xi^2 \omega^3 b}{27\rho_{0w} c_w^2 \rho_{0f}^2 c_f a^2} \right) \left(1 - \frac{a^3}{b^3} \right) - \left(\frac{\xi^2 \omega^3 b}{3\rho_{0f}^3 c_f^3 a^2} \right) + \left[\frac{c_f(\gamma_a - 1)}{\rho_{0f} b^2} \right] \left(\frac{\omega \kappa_a}{2\rho_{0a} c_{pa}} \right)^{1/2} \\
& + \left[\frac{2c_f s b(\gamma_a - 1)}{3\rho_{0w} c_w^2 \rho_{0f} a^4} \right] \left(\frac{\omega \kappa_a}{2\rho_{0a} c_{pa}} \right)^{1/2} + \left[\frac{\omega^2 c_f b(\gamma_a - 1)}{3\rho_{0w} c_w^2 a} \right] \left(\frac{\omega \kappa_a}{2\rho_{0a} c_{pa}} \right)^{1/2} \left(1 - \frac{a}{b} \right) \\
& + \left[\frac{2s b(\gamma_a - 1)}{3\rho_{0f}^2 c_f a^4} \right] \left(\frac{\omega \kappa_a}{2\rho_{0a} c_{pa}} \right)^{1/2} \left(1 - \frac{a^3}{b^3} \right) - \left[\frac{\omega^2 b(\gamma_a - 1)}{3\rho_{0f} c_f a} \right] \left(\frac{\omega \kappa_a}{2\rho_{0a} c_{pa}} \right)^{1/2} \\
& + \left[\frac{\omega^3 \xi \kappa_a b(\gamma_a - 1)}{18\rho_{0w} c_w^2 \rho_{0f}^2 c_f c_{pa} a^2} \right] \left[1 + \left(\frac{2s}{\omega a^2} \right) \left(\frac{c_{pa}}{2\rho_{0a} \omega \kappa_a} \right)^{1/2} \right] \left(11 + \frac{4a^3}{b^3} \right)
\end{aligned}$$

$$\begin{aligned}
& + \left[\frac{11\omega^2\xi^2b(\gamma_a-1)}{9\rho_{0w}c_w^2\rho_{0f}^2c_f a^3} \right] \left(\frac{\omega\kappa_a}{2\rho_{0a}c_{pa}} \right)^{1/2} \left(1 - \frac{a^3}{b^3} \right) \\
& - \left[\frac{2\omega\xi c_f b(\gamma_a-1)}{3\rho_{0w}c_w^2\rho_{0f} a^3} \right] \left(\frac{\omega\kappa_a}{2\rho_{0a}c_{pa}} \right)^{1/2} \left(1 - \frac{a^3}{b^3} \right) \\
& - \left[\frac{\omega^3\xi\kappa_a b(\gamma_a-1)}{2\rho_{0f}^3c_f^3c_{pa}a^2} \right] \left[1 + \left(\frac{2s}{\omega a^2} \right) \left(\frac{c_{pa}}{2\rho_{0a}\omega\kappa_a} \right)^{1/2} \right] \left(1 - \frac{a^3}{b^3} \right) \\
& - \left[\frac{\omega^2\xi^2b(\gamma_a-1)}{\rho_{0f}^3c_f^3a^3} \right] \left(\frac{\omega\kappa_a}{2\rho_{0a}c_{pa}} \right)^{1/2} + \left[\frac{\omega\xi(\gamma_a-1)}{6\rho_{0f}^2c_f b^2} \right] \left(\frac{\omega\kappa_a}{2\rho_{0a}c_{pa}} \right)^{1/2} \left(11 + \frac{4b^3}{a^3} \right) \\
& + i \left(\frac{\rho_{0a}c_a^2\omega^2\xi b}{18\rho_{0w}c_w^2\rho_{0f}^2c_f a^2} \right) \left(1 - \frac{2s}{3\rho_{0a}c_a^2a} \right) \left(11 + \frac{4a^3}{b^3} \right) \\
& + i \left(\frac{2\omega^2\xi c_f b}{9\rho_{0w}c_w^2\rho_{0f} a^2} \right) \left(1 - \frac{a^3}{b^3} \right) - i \left(\frac{\omega\xi a}{18\rho_{0f}^2c_f b^2} \right) \left(11 + \frac{4b^3}{a^3} \right) \\
& - i \left(\frac{\rho_{0a}c_a^2\omega^2\xi b}{2\rho_{0f}^3c_f^3a^2} \right) \left(1 - \frac{2s}{3\rho_{0a}c_a^2a} \right) \left(1 - \frac{a^3}{b^3} \right) \\
& + i \left[\frac{c_f(\gamma_a-1)}{\rho_{0f}b^2} \right] \left(\frac{\omega\kappa_a}{2\rho_{0a}c_{pa}} \right)^{1/2} - i \left[\frac{\omega^2b(\gamma_a-1)}{3\rho_{0f}c_f a} \right] \left(\frac{\omega\kappa_a}{2\rho_{0a}c_{pa}} \right)^{1/2} \\
& + i \left[\frac{\omega^2c_f b(\gamma_a-1)}{3\rho_{0w}c_w^2a} \right] \left(\frac{\omega\kappa_a}{2\rho_{0a}c_{pa}} \right)^{1/2} \left(1 - \frac{a}{b} \right) \\
& + i \left[\frac{\omega^2c_f\kappa_a b(\gamma_a-1)}{3\rho_{0w}c_w^2c_{pa}a^2\rho_{0f}} \right] \left[1 + \left(\frac{2s}{\omega a^2} \right) \left(\frac{c_{pa}}{2\rho_{0a}\omega\kappa_a} \right)^{1/2} \right] \\
& - i \left[\frac{\omega^2\kappa_a b(\gamma_a-1)}{3\rho_{0f}^2c_f c_{pa}a^2} \right] \left[1 + \left(\frac{2s}{\omega a^2} \right) \left(\frac{c_{pa}}{2\rho_{0a}\omega\kappa_a} \right)^{1/2} \right] \left(1 - \frac{a^3}{b^3} \right) \\
& - i \left[\frac{\omega\xi s b(\gamma_a-1)}{9\rho_{0w}c_w^2\rho_{0f}^2c_f a^4} \right] \left(\frac{\omega\kappa_a}{2\rho_{0a}c_{pa}} \right)^{1/2} \left(11 + \frac{4a^3}{b^3} \right) \\
& + i \left[\frac{2\omega\xi c_f b(\gamma_a-1)}{3\rho_{0w}c_w^2\rho_{0f} a^3} \right] \left(\frac{\omega\kappa_a}{2\rho_{0a}c_{pa}} \right)^{1/2} \left(1 - \frac{a^3}{b^3} \right) \\
& + i \left[\frac{11\omega^2\xi^2b(\gamma_a-1)}{9\rho_{0w}c_w^2\rho_{0f}^2c_f a^3} \right] \left(\frac{\omega\kappa_a}{2\rho_{0a}c_{pa}} \right)^{1/2} \left(1 - \frac{a^3}{b^3} \right) \\
& + i \left[\frac{\omega\xi s b(\gamma_a-1)}{\rho_{0f}^3c_f^3a^3} \right] \left(\frac{\omega\kappa_a}{2\rho_{0a}c_{pa}} \right)^{1/2} \left(1 - \frac{a^3}{b^3} \right) \\
& - i \left[\frac{\omega\xi(\gamma_a-1)}{6\rho_{0f}^2c_f b^2} \right] \left(\frac{\omega\kappa_a}{2\rho_{0a}c_{pa}} \right)^{1/2} \left(11 + \frac{4b^3}{a^3} \right) - i \left[\frac{\omega^2\xi^2b(\gamma_a-1)}{\rho_{0f}^3c_f^3a^3} \right] \left(\frac{\omega\kappa_a}{2\rho_{0a}c_{pa}} \right)^{1/2}
\end{aligned}$$

(B-57)

Substitution of equations B-55 and B-56 into B-50 yields:

$$\begin{aligned}
 (\rho_{0a} c_a^2) Z = & - \left(\frac{\rho_{0a} c_a^2 \xi c_w}{6 \omega \rho_{0w} \rho_{0f}^2 c_f a^2 b^2} \right) \left(1 - \frac{2s}{3 \rho_{0a} c_a^2 a} \right) \left(11 + \frac{4a^3}{b^3} \right) \\
 & - \left(\frac{2 \xi c_w c_f}{3 \omega \rho_{0w} \rho_{0f} a^2 b^2} \right) \left(1 - \frac{a^3}{b^3} \right) + \left(\frac{\omega \xi c_w a}{18 \rho_{0f}^2 c_f b^3} \right) \left(11 + \frac{4b^3}{a^3} \right) \\
 & + \left(\frac{\rho_{0a} c_a^2 \omega \xi c_w}{2 \rho_{0f}^3 c_f^3 a^2} \right) \left(1 - \frac{2s}{3 \rho_{0a} c_a^2 a} \right) \left(1 - \frac{a^3}{b^3} \right) + \left[\frac{\omega c_w (Y_a - 1)}{3 \rho_{0f} c_f a} \right] \left(\frac{\omega \kappa_a}{2 \rho_{0a} c_{pa}} \right)^{1/2} \\
 & - \left[\frac{c_w c_f (Y_a - 1)}{\omega \rho_{0f} b^3} \right] \left(\frac{\omega \kappa_a}{2 \rho_{0a} c_{pa}} \right)^{1/2} - \left[\frac{c_w c_f (Y_a - 1)}{\omega \rho_{0w} a b^2} \right] \left(\frac{\omega \kappa_a}{2 \rho_{0a} c_{pa}} \right)^{1/2} \left(1 - \frac{a}{b} \right) \\
 & - \left[\frac{c_w c_f \kappa_a (Y_a - 1)}{\omega \rho_{0w} \rho_{0f} c_{pa} a^2 b^2} \right] \left[1 + \left(\frac{2s}{\omega a^2} \right) \left(\frac{c_{pa}}{2 \rho_{0a} \omega \kappa_a} \right)^{1/2} \right] \\
 & + \left[\frac{\omega c_w \kappa_a (Y_a - 1)}{3 \rho_{0f}^2 c_f c_{pa} a^2} \right] \left[1 + \left(\frac{2s}{\omega a^2} \right) \left(\frac{c_{pa}}{2 \rho_{0a} \omega \kappa_a} \right)^{1/2} \right] \left(1 - \frac{a^3}{b^3} \right) \\
 & + \left[\frac{\xi c_w s (Y_a - 1)}{3 \omega^2 \rho_{0w} \rho_{0f}^2 c_f a^4 b^2} \right] \left(\frac{\omega \kappa_a}{2 \rho_{0a} c_{pa}} \right)^{1/2} \left(11 + \frac{4a^3}{b^3} \right) \\
 & - \left[\frac{2 \xi c_w c_f (Y_a - 1)}{\omega^2 \rho_{0w} \rho_{0f} a^3 b^2} \right] \left(\frac{\omega \kappa_a}{2 \rho_{0a} c_{pa}} \right)^{1/2} \left(1 - \frac{a^3}{b^3} \right) \\
 & - \left[\frac{11 \xi^2 c_w (Y_a - 1)}{3 \rho_{0w} \rho_{0f}^2 c_f a^3 b^2} \right] \left(\frac{\omega \kappa_a}{2 \rho_{0a} c_{pa}} \right)^{1/2} \left(1 - \frac{a^3}{b^3} \right) \\
 & - \left[\frac{\xi c_w s (Y_a - 1)}{\rho_{0f}^3 c_f^3 a^4} \right] \left(\frac{\omega \kappa_a}{2 \rho_{0a} c_{pa}} \right)^{1/2} \left(1 - \frac{a^3}{b^3} \right) \\
 & + \left[\frac{\xi c_w (Y_a - 1)}{6 \rho_{0f}^2 c_f b^3} \right] \left(\frac{\omega \kappa_a}{2 \rho_{0a} c_{pa}} \right)^{1/2} \left(11 + \frac{4b^3}{a^3} \right) \\
 & + \left[\frac{\omega \xi^2 c_w (Y_a - 1)}{\rho_{0f}^3 c_f^3 a^3} \right] \left(\frac{\omega \kappa_a}{2 \rho_{0a} c_{pa}} \right)^{1/2} - i \left(\frac{\rho_{0a} c_a^2 c_w c_f}{\omega^2 \rho_{0w} \rho_{0f} a^2 b^2} \right) \left(1 - \frac{2s}{3 \rho_{0a} c_a^2 a} \right) \\
 & + i \left(\frac{c_w c_f}{3 \rho_{0w} b^2} \right) \left(1 - \frac{a}{b} \right) + i \left(\frac{\rho_{0a} c_a^2 c_w}{3 \rho_{0f}^2 c_f a^2} \right) \left(1 - \frac{2s}{3 \rho_{0a} c_a^2 a} \right) \left(1 - \frac{a^3}{b^3} \right) \\
 & - i \left(\frac{\omega^2 c_w}{9 \rho_{0f} c_f} \right) + i \left(\frac{c_w c_f a}{3 \rho_{0f} b^3} \right) + i \left(\frac{11 \xi^2 c_w}{9 \rho_{0w} \rho_{0f}^2 c_f a^2 b^2} \right) \left(1 - \frac{a^3}{b^3} \right) - i \left(\frac{\omega^2 \xi^2 c_w}{3 \rho_{0f}^3 c_f^3 a^2} \right)
 \end{aligned}$$

$$\begin{aligned}
& + i \left[\frac{c_w c_t (Y_a - 1)}{\omega \rho_{0t} b^3} \right] \left(\frac{\omega \kappa_a}{2 \rho_{0a} c_{pa}} \right)^{1/2} - i \left[\frac{\omega c_w (Y_a - 1)}{3 \rho_{0t} c_t a} \right] \left(\frac{\omega \kappa_a}{2 \rho_{0a} c_{pa}} \right)^{1/2} \\
& + i \left[\frac{2 c_w c_t s (Y_a - 1)}{\omega^3 \rho_{0t} \rho_{0w} a^4 b^2} \right] \left(\frac{\omega \kappa_a}{2 \rho_{0a} c_{pa}} \right)^{1/2} - i \left[\frac{2 c_w s (Y_a - 1)}{3 \omega \rho_{0t}^2 c_t a^4} \right] \left(\frac{\omega \kappa_a}{2 \rho_{0a} c_{pa}} \right)^{1/2} \left(1 - \frac{a^3}{b^3} \right) \\
& + i \left[\frac{c_w c_t (Y_a - 1)}{\omega \rho_{0w} a b^2} \right] \left(\frac{\omega \kappa_a}{2 \rho_{0a} c_{pa}} \right)^{1/2} \left(1 - \frac{a}{b} \right) \\
& + i \left[\frac{\xi c_w \kappa_a (Y_a - 1)}{6 \rho_{0w} \rho_{0t}^2 c_t c_{pa} a^2 b^2} \right] \left[1 + \left(\frac{2s}{\omega a^2} \right) \left(\frac{c_{pa}}{2 \rho_{0a} \omega \kappa_a} \right)^{1/2} \right] \left(11 + \frac{4a^3}{b^3} \right) \\
& + i \left[\frac{11 \xi^2 c_w (Y_a - 1)}{3 \omega \rho_{0w} \rho_{0t}^2 c_t a^3 b^2} \right] \left(\frac{\omega \kappa_a}{2 \rho_{0a} c_{pa}} \right)^{1/2} \left(1 - \frac{a^3}{b^3} \right) \\
& - i \left[\frac{2 \xi c_w c_t (Y_a - 1)}{\omega^2 \rho_{0w} \rho_{0t} a^3 b^2} \right] \left(\frac{\omega \kappa_a}{2 \rho_{0a} c_{pa}} \right)^{1/2} \left(1 - \frac{a^3}{b^3} \right) \\
& - i \left[\frac{\omega^2 \xi c_w \kappa_a (Y_a - 1)}{2 \rho_{0t}^3 c_t^3 c_{pa} a^2} \right] \left[1 + \left(\frac{2s}{\omega a^2} \right) \left(\frac{c_{pa}}{2 \rho_{0a} \omega \kappa_a} \right)^{1/2} \right] \left(1 - \frac{a^3}{b^3} \right) \\
& - i \left[\frac{\omega \xi^2 c_w (Y_a - 1)}{\rho_{0t}^3 c_t^3 a^3} \right] \left(\frac{\omega \kappa_a}{2 \rho_{0a} c_{pa}} \right)^{1/2} + i \left[\frac{\xi c_w (Y_a - 1)}{6 \rho_{0t}^2 c_t b^3} \right] \left(\frac{\omega \kappa_a}{2 \rho_{0a} c_{pa}} \right)^{1/2} \left(11 + \frac{4b^3}{a^3} \right).
\end{aligned}$$

(B-58)

The terms in equations B-57 and B-58 have been arranged so that the real and imaginary inertial, viscous, thermal, and viscothermal terms are grouped. These terms will be designed as the m-, ξ -, q-, ξq -, im-, $i\xi$ -, iq-, and $i\xi q$ -terms, respectively. In equation B-57, the first five terms are m-terms. These are followed by two ξ -terms, five q-terms, six ξq -terms, four $i\xi$ -terms, five iq-terms, and six $i\xi q$ -terms. In equation B-58, the first four terms are ξ -terms. These are followed by five q-terms, six ξq -terms, five im-terms, two $i\xi$ -terms, five iq-terms, and six $i\xi q$ -terms.

The next step is to simplify each group of terms for Y and (Y-Z). However, examinations of equations B-57 and B-58 indicates that the powers of the parameters in the Y and Z terms are never identical. Thus, the terms in Z can be examined independently of Y, since the subtraction of Z from Y can not result in the reduction in the order of magnitude of any terms. After each group of terms is compared and simplified, the expressions for Y and Z will be further simplified by comparing all remaining terms. Then the subtraction (Y-Z) will be performed and that expression simplified.

Comparison of the terms within the groups in equation B-57 yields:

$$(\rho_{0a} c_a^2) Y = \left(\frac{\omega c_t a}{3 \rho_{0t} b^2} \right) + \left(\frac{\omega^3 \xi^2 b}{3 \rho_{0t}^3 c_t^3 a^2} \right) \left[\frac{11 \rho_{0t} c_t^2}{9 \rho_{0w} c_w^2} \left(1 - \frac{a^3}{b^3} \right) - 1 \right]$$

$$\begin{aligned}
& + \left[\frac{c_t(Y_a - 1)}{\rho_{0t} b^2} \right] \left(\frac{\omega \kappa_a}{2 \rho_{0a} c_{pa}} \right)^{1/2} \\
& + \left[\frac{\omega \xi b (Y_a - 1)}{\rho_{0t}^2 c_t a^3} \right] \left(\frac{\omega \kappa_a}{2 \rho_{0a} c_{pa}} \right)^{1/2} \left\{ \frac{2}{3} \left(1 - \frac{\rho_{0t} c_t^2}{\rho_{0w} c_w^2} \right) \right. \\
& + \left(\frac{a^3}{6 b^3} \right) \left(11 + 4 \frac{\rho_{0t} c_t^2}{\rho_{0w} c_w^2} \right) + \left(\frac{\omega \xi}{\rho_{0t} c_t^2} \right) \left(\frac{11 \rho_{0t} c_t^2}{9 \rho_{0w} c_w^2} - 1 \right) \Big\} \\
& + i \left(\frac{\omega^2 \xi b}{\rho_{0t}^2 c_t a^2} \right) \left\{ \left(\frac{\rho_{0a} c_a^2}{\rho_{0t} c_t^2} \right) \left[\left(\frac{11 \rho_{0t} c_t^2}{9 \rho_{0w} c_w^2} - 1 \right) + \left(\frac{4 \rho_{0t} c_t^2}{9 \rho_{0w} c_w^2} + 1 \right) \left(\frac{a^3}{b^3} \right) \right] \right. \\
& + \frac{2}{9} \left[\left(\frac{\rho_{0t} c_t^2}{\rho_{0w} c_w^2} - 1 \right) - \left(\frac{\rho_{0t} c_t^2}{\rho_{0w} c_w^2} + \frac{11}{4} \right) \left(\frac{a^3}{b^3} \right) \right] \Big\} + i \left[\frac{c_t(Y_a - 1)}{\rho_{0t} b^2} \right] \left(\frac{\omega \kappa_a}{2 \rho_{0a} c_{pa}} \right)^{1/2} \\
& + i \left[\frac{\omega \xi b (Y_a - 1)}{\rho_{0t}^2 c_t a^3} \right] \left(\frac{\omega \kappa_a}{2 \rho_{0a} c_{pa}} \right)^{1/2} \left\{ \frac{2}{3} \left[\left(\frac{\rho_{0t} c_t^2}{\rho_{0w} c_w^2} - 1 \right) \right. \right. \\
& - \left. \left(\frac{\rho_{0t} c_t^2}{\rho_{0w} c_w^2} + \frac{11}{4} \right) \left(\frac{a^3}{b^3} \right) \right] \\
& + \left. \left(\frac{\xi \omega}{\rho_{0t} c_t^2} \right) \left[\left(\frac{11 \rho_{0t} c_t^2}{9 \rho_{0w} c_w^2} - 1 \right) - \left(\frac{11 \rho_{0t} c_t^2}{9 \rho_{0w} c_w^2} \right) \left(\frac{a^3}{b^3} \right) \right] \right\}. \quad (B-59)
\end{aligned}$$

Then a comparison of all terms in equation B-59 yields:

$$\begin{aligned}
\left(\frac{\rho_{0t} \rho_{0a} c_a^2}{c_t} \right) Y &= \left(\frac{\omega a}{3 b^2} \right) \left[1 + \left(\frac{\omega^2 \xi^2 b^3}{\rho_{0t}^2 c_t^4 a^3} \right) \left(\frac{11 \rho_{0t} c_t^2}{9 \rho_{0w} c_w^2} - 1 \right) \right] \\
& + i \left(\frac{\omega^2 \xi b}{2 \rho_{0t} c_t^2 a^2} \right) \left\{ \left(\frac{\rho_{0a} c_a^2}{\rho_{0t} c_t^2} \right) \left[\left(\frac{11 \rho_{0t} c_t^2}{9 \rho_{0w} c_w^2} - 1 \right) + \left(\frac{4 \rho_{0t} c_t^2}{9 \rho_{0w} c_w^2} + 1 \right) \left(\frac{a^3}{b^3} \right) \right] \right. \\
& + \frac{4}{9} \left[\left(\frac{\rho_{0t} c_t^2}{\rho_{0w} c_w^2} - 1 \right) - \left(\frac{\rho_{0t} c_t^2}{\rho_{0w} c_w^2} + \frac{11}{4} \right) \left(\frac{a^3}{b^3} \right) \right] \Big\} + i \left[\frac{(Y_a - 1)}{b^2} \right] \left(\frac{\omega \kappa_a}{2 \rho_{0a} c_{pa}} \right)^{1/2}. \quad (B-60)
\end{aligned}$$

Comparison of the terms within groups in equation B-58 yields:

$$(\rho_{0a} c_a^2) Z = - \left(\frac{2 \xi c_w c_t}{3 \omega \rho_{0w} \rho_{0t} a^2 b^2} \right) + \left[\frac{c_w c_t (Y_a - 1)}{\omega \rho_{0w} a b^2} \right] \left(\frac{\omega \kappa_a}{2 \rho_{0a} c_{pa}} \right)^{1/2} \left(1 + \frac{2s}{\rho_{0t} \omega^2 a^5} \right)$$

$$\begin{aligned}
& - \left[\frac{2\xi c_w c_f (Y_a - 1)}{\omega^2 \rho_{0w} \rho_{0f} a^3 b^2} \right] \left(\frac{\omega \kappa_a}{2\rho_{0a} c_{pa}} \right)^{1/2} \left(1 - \frac{11\omega\xi}{6\rho_{0f} c_f^2} \right) \\
& + i \left(\frac{c_w c_f}{3\rho_{0w} b^2} \right) \left[\left(\frac{3\rho_{0a} c_a^2}{\rho_{0f} \omega^2 a^2} \right) \left(1 - \frac{2s}{3\rho_{0a} c_a^2 a} \right) - 1 \right] \\
& + i \left(\frac{11\xi^2 c_w}{9\rho_{0w} \rho_{0f}^2 c_f^2 a^2 b^2} \right) + i \left[\frac{c_w c_f (Y_a - 1)}{\omega \rho_{0w} a b^2} \right] \left(\frac{\omega \kappa_a}{2\rho_{0a} c_{pa}} \right)^{1/2} \left(1 + \frac{2s}{\rho_{0f} \omega^2 a^3} \right) \\
& - i \left[\frac{2\xi c_w c_f (Y_a - 1)}{\omega^2 \rho_{0w} \rho_{0f} a^3 b^2} \right] \left(\frac{\omega \kappa_a}{2\rho_{0a} c_{pa}} \right)^{1/2} \left(1 - \frac{11\omega\xi}{6\rho_{0f} c_f^2} \right) \quad (B-61)
\end{aligned}$$

Then a comparison of all terms in equation B-61 yields:

$$\begin{aligned}
\left(\frac{\rho_{0f} \rho_{0a} c_a^2}{c_f} \right) Z = & - \left(\frac{2\xi c_w}{3\omega \rho_{0w} a^2 b^2} \right) - \left[\frac{c_w \rho_{0f} (Y_a - 1)}{\omega \rho_{0w} a b^2} \right] \left(\frac{\omega \kappa_a}{2\rho_{0a} c_{pa}} \right)^{1/2} \left(1 + \frac{2s}{\rho_{0f} \omega^2 a^3} \right) \\
& - i \left(\frac{c_w \rho_{0f}}{3\rho_{0w} b^2} \right) \left[\left(\frac{3\rho_{0a} c_a^2}{\rho_{0f} \omega^2 a^2} \right) \left(1 - \frac{2s}{3\rho_{0a} c_a^2 a} \right) - 1 \right] \\
& + i \left(\frac{11\xi^2 c_w}{9\rho_{0w} \rho_{0f} c_f^2 a^2 b^2} \right) + i \left[\frac{c_w \rho_{0f} (Y_a - 1)}{\omega \rho_{0w} a b^2} \right] \left(\frac{\omega \kappa_a}{2\rho_{0a} c_{pa}} \right)^{1/2} \left(1 + \frac{2s}{\rho_{0f} \omega^2 a^3} \right) \quad (B-62)
\end{aligned}$$

Examination of equations B-60 and B-62 shows that all the viscothermal terms are negligible. Subtraction of equation B-62 from B-60 and a subsequent comparison of terms yields:

$$\begin{aligned}
\left(\frac{\rho_{0f} \rho_{0a} c_a^2}{c_f} \right) (Y - Z) = & \left(\frac{\omega a}{3b^2} \right) \left\{ 1 + \left(\frac{2\xi c_w}{\rho_{0w} \omega^2 a^3} \right) \right. \\
& + \left. \left[\frac{3\rho_{0f} c_w (Y_a - 1)}{\rho_{0w} \omega^2 a^2} \right] \left(\frac{\omega \kappa_a}{2\rho_{0a} c_{pa}} \right)^{1/2} \left(1 + \frac{2s}{\rho_{0f} \omega^2 a^3} \right) \right\} \\
& + i \left(\frac{c_w}{3\rho_{0w} b^2} \right) \left[\left(\frac{3\rho_{0a} c_a^2}{\omega^2 a^2} \right) \left(1 - \frac{2s}{3\rho_{0a} c_a^2 a} \right) - \rho_{0f} - \left(\frac{11\xi^2}{3\rho_{0f} c_f^2 a^2} \right) \right] \quad (B-63)
\end{aligned}$$

Equation III-32 indicates that $|B_w|^2$ is required to determine σ . This implies, from equation B-48, that $|Y|^2$ is required. If

$$Y = Y_r + iY_i \quad (B-64)$$

then

$$|Y|^2 = Y_r^2 + Y_i^2 \quad (B-65)$$

where Y_r and Y_i are the real and imaginary parts of Y , respectively. Thus, in light of equation B-65, it is possible to simplify equation B-60 by comparing magnitudes of real and imaginary terms. This comparison yields:

$$\left(\frac{\rho_{0f} \rho_{0a} c_a^2}{c_f} \right) Y = \left(\frac{\omega a}{3b^2} \right) [1 + \Lambda + i\lambda] \quad (B-66)$$

where

$$\Lambda = \left(\frac{\omega^2 \xi^2 b^3}{\rho_{0f}^2 c_f^4 a^3} \right) \left(\frac{11 \rho_{0f} c_f^2}{9 \rho_{0w} c_w^2} - 1 \right) \quad (\text{B-67})$$

and

$$\lambda = \left(\frac{2 \omega \xi b^3}{3 \rho_{0f} c_f^2 a^3} \right) \left[\left(\frac{\rho_{0f} c_f^2}{\rho_{0w} c_w^2} - 1 \right) - \left(\frac{\rho_{0f} c_f^2}{\rho_{0w} c_w^2} + \frac{11}{4} \right) \left(\frac{a^3}{b^3} \right) \right] \quad (\text{B-68})$$

This set of equations does not give Y_i , and therefore B_w , to the desired accuracy of ten percent, but it is sufficiently accurate in the final answer for $|B_w|^2$.

Thus, the simplification process of equation III-16 yields:

$$\begin{aligned} \frac{B_w}{A} = & - \left[1 + \Lambda + i\lambda \right] \left\{ 1 + \left(\frac{2 \xi c_w}{\rho_{0w} \omega^2 a^3} \right) \right. \\ & + \left[\frac{3 \rho_{0f} c_w (\gamma_a - 1)}{\rho_{0w} \omega^2 a^2} \right] \left(\frac{\omega \kappa_a}{2 \rho_{0a} c_{pa}} \right)^{1/2} \left(1 + \frac{2s}{\rho_{0f} \omega^2 a^3} \right) \\ & \left. + i \left(\frac{c_w \rho_{0f}}{\rho_{0w} \omega a} \right) \left[\left(\frac{3 \rho_{0a} c_a^2}{\rho_{0f} \omega^2 a^2} \right) \left(1 - \frac{2s}{3 \rho_{0a} c_a^2 a} \right) - 1 - \left(\frac{11 \xi^2}{3 \rho_{0f}^2 c_f^2 a^2} \right) \right] \right\}^{-1}, \quad (\text{B-69}) \end{aligned}$$

where Λ and λ are given by equations B-67 and B-68.

UNCLASSIFIED

SECURITY CLASSIFICATION OF THIS PAGE (When Data Entered)

REPORT DOCUMENTATION PAGE		READ INSTRUCTIONS BEFORE COMPLETING FORM
1. REPORT NUMBER NORDA REPORT #4	2. GOVT ACCESSION NO.	3. RECIPIENT'S CATALOG NUMBER
4. TITLE (and Subtitle) A NEW MODEL OF RESONANT ACOUSTIC SCATTERING BY SWIMBLADDER-BEARING FISH		5. TYPE OF REPORT & PERIOD COVERED FINAL
7. AUTHOR(s) RICHARD H. LOVE		6. PERFORMING ORG. REPORT NUMBER
9. PERFORMING ORGANIZATION NAME AND ADDRESS NAVAL OCEAN RESEARCH AND DEVELOPMENT ACTIVITY NSTL STATION, MISSISSIPPI 39529		8. CONTRACT OR GRANT NUMBER(s)
11. CONTROLLING OFFICE NAME AND ADDRESS NAVAL OCEAN RESEARCH AND DEVELOPMENT ACTIVITY NSTL STATION, MISSISSIPPI 39529		10. PROGRAM ELEMENT, PROJECT, TASK AREA & WORK UNIT NUMBERS 62759N/2550/301
14. MONITORING AGENCY NAME & ADDRESS (if different from Controlling Office)		12. REPORT DATE AUGUST 1977
		13. NUMBER OF PAGES 12
		15. SECURITY CLASS. (of this report) UNCLASSIFIED
		15a. DECLASSIFICATION/DOWNGRADING SCHEDULE
16. DISTRIBUTION STATEMENT (of this Report) APPROVED FOR PUBLIC RELEASE: DISTRIBUTION UNLIMITED		
17. DISTRIBUTION STATEMENT (of the abstract entered in Block 20, if different from Report)		
18. SUPPLEMENTARY NOTES		
19. KEY WORDS (Continue on reverse side if necessary and identify by block number) VOLUME SCATTERING, BIOLOGICAL SCATTERING, ACOUSTIC MODELS, BIOACOUSTIC MODELS, REVERBERATION		
20. ABSTRACT (Continue on reverse side if necessary and identify by block number) The primary cause of oceanic volume reverberation is resonant scattering by the swimbladders of small fish. A new model of a swimbladder-bearing fish has been developed in order to provide improved predictions of the resonant frequency and acoustic cross section of such a fish. Development of a new model was undertaken because comparisons of the predictions of previous models with experimental data show these models to be inadequate. Primarily, the experimental data indicate that damping in fish tissue is consistently greater		

DD FORM 1473
1 JAN 73EDITION OF 1 NOV 65 IS OBSOLETE
S/N 0102-014-6601

UNCLASSIFIED

SECURITY CLASSIFICATION OF THIS PAGE (When Data Entered)

392773

20.

than that predicted by previous models. In addition, in several instances, resonant frequencies have been measured which are significantly higher than can be accounted for by these models.

The new model consists of a small, spherical shell, enclosing an air cavity, in water. The shell is a viscous, heat-conducting Newtonian fluid, with the physical properties of fish flesh. The interface between the shell and the cavity supports a surface tension. The shell is insonified by a harmonic plane compressional wave, whose wave-length is large compared to the shell diameter.

The solution to the problem consists of obtaining the amplitude of the scattered compressional wave. This was accomplished by first determining the appropriate wave equations from the linearized equations of motion. Eigenfunction solutions to these equations were then obtained. However, theoretical evidence indicates that only the fundamental mode is an important contributor to volume reverberation, so that higher modes were neglected. Application of the boundary conditions then led to the required solution for the amplitude of the scattered compressional wave. Due to the complexity of this solution, order of magnitude analyses of the various terms were conducted in order to obtain a simplified expression. Equations for both the resonant frequency and acoustic cross section were then determined from this simplified expression.

A comparison of the results of the new model with experimental data indicates that the new model constitutes a definite improvement over previous models. The new model can predict the high values of damping and elevated resonant frequencies that previous models could not. The comparison indicates that the model is most accurate for fish in which tension in the swimbladder wall has a minor effect on resonant scattering. This includes the fish which are of interest in studies of volume reverberation and therefore, the new model will be of considerable value in such studies.